AGU PUBLICATIONS

JGR

Journal of Geophysical Research: Earth Surface

RESEARCH ARTICLE
10.1002/2017JF004236

Key Points:
- The available information on earthquake-induced landslide data is cataloged
- The quality, completeness, and representation of earthquake-induced landslide inventories are discussed
- A scoring method for an overall evaluation of earthquake-induced landslide inventories is proposed

Supporting Information:
- Supporting Information S1
- Table S1

Correspondence to:
H. Tanyaş,
h.tanyas@utwente.nl

Citation:
Tanyaş, H., van Westen, C. J., Allstadt, K. E., Anna Nowicki Jessee, M., Görüm, T., Jibson, R. W., … Hovius, N. (2017). Presentation and analysis of a worldwide database of earthquake-induced landslide inventories. *Journal of Geophysical Research: Earth Surface*, *122*, 1991–2015. https://doi.org/10.1002/2017JF004236

Received 30 JAN 2017
Accepted 20 AUG 2017
Accepted article online 24 SEP 2017
Published online 30 OCT 2017

Presentation and Analysis of a Worldwide Database of Earthquake-Induced Landslide Inventories

Hakan Tanyaş[1], Cees J. van Westen[1], Kate E. Allstadt[2], M. Anna Nowicki Jessee[3], Tolga Görüm[4], Randall W. Jibson[2], Jonathan W. Godt[2], Hiroshi P. Sato[5], Robert G. Schmitt[2], Odin Marc[6,8], and Niels Hovius[7,8]

[1]Faculty of Geo-Information Science and Earth Observation, University of Twente, Enschede, Netherlands, [2]U.S. Geological Survey, Golden, CO, USA, [3]Indiana University Bloomington, Bloomington, IN, USA, [4]Department of Geography, Istanbul University, Istanbul, Turkey, [5]Department of Geography, Nihon University, Tokyo, Japan, [6]Now at Institut de Physique du Globe Strasbourg, University of Strasbourg, EOST, Strasbourg, France, [7]Institute of Earth and Environmental Science, University of Potsdam, Potsdam, Germany, [8]Helmholtz Centre Potsdam, German Research Center for Geosciences, Potsdam, Germany

Abstract Earthquake-induced landslide (EQIL) inventories are essential tools to extend our knowledge of the relationship between earthquakes and the landslides they can trigger. Regrettably, such inventories are difficult to generate and therefore scarce, and the available ones differ in terms of their quality and level of completeness. Moreover, access to existing EQIL inventories is currently difficult because there is no centralized database. To address these issues, we compiled EQIL inventories from around the globe based on an extensive literature study. The database contains information on 363 landslide-triggering earthquakes and includes 66 digital landslide inventories. To make these data openly available, we created a repository to host the digital inventories that we have permission to redistribute through the U.S. Geological Survey ScienceBase platform. It can grow over time as more authors contribute their inventories. We analyze the distribution of EQIL events by time period and location, more specifically breaking down the distribution by continent, country, and mountain region. Additionally, we analyze frequency distributions of EQIL characteristics, such as the approximate area affected by landslides, total number of landslides, maximum distance from fault rupture zone, and distance from epicenter when the fault plane location is unknown. For the available digital EQIL inventories, we examine the underlying characteristics of landslide size, topographic slope, roughness, local relief, distance to streams, peak ground acceleration, peak ground velocity, and Modified Mercalli Intensity. Also, we present an evaluation system to help users assess the suitability of the available inventories for different types of EQIL studies and model development.

1. Introduction

Losses due to earthquake-triggered landslides can be significant, and for some events they exceed losses directly due to shaking (Bird & Bommer, 2004; Harp et al., 1984). Approximately 70% of all earthquake-related casualties not caused by ground shaking are caused by landslides (Marano et al., 2010). From 2004 to 2010 a total of 47,736 earthquake-induced landslide (EQIL) casualties were reported (Kennedy et al., 2015; Petley, 2012). In addition, EQIL commonly have considerable indirect and long-term effects on society and infrastructure that intensify their overall damage (e.g., Huang & Fan, 2013; Shafique et al., 2016) such as blocked roads that hamper medical care (Marui & Nadim, 2009), floods from the failure of landslide dams, increased debris-flow activity (e.g., Shieh et al., 2009; Tang et al., 2016), and downstream river aggradation and associated flooding (e.g., Korup, 2006).

Papers having both worldwide (Keefer, 1984; Rodriguez et al., 1999) and national (Hancox et al., 2002; Papadopoulos & Plessa, 2000; Prestininzi & Romeo, 2000) perspectives have established a baseline for understanding the relations among EQIL distributions, landslide types, and areas of coverage. However, several authors have demonstrated that these relationships have high uncertainty, and they are not always valid (e.g. Barlow et al., 2014; Gorum et al., 2014; Hancox et al., 2002; Jibson et al., 2004; Jibson & Harp, 2012). A number of explanations have been given to explain this uncertainty. Hancox et al. (2002) stated that the data used to derive these relationships might be inadequate to characterize the whole world, as the work by Keefer (1984) was based predominantly on earthquakes in North America, and data sets belonging to different climatic, geologic, and topographic conditions may give different results. Jibson and Harp (2012) found

that landslide distance limits differ between plate boundary earthquakes, which made up most of Keefer's (1984) data set, and intraplate earthquakes, where seismic wave attenuation is generally much lower. Furthermore, Gorum et al. (2014) concluded that estimating the number of coseismic landslides from earthquake magnitude alone remains highly problematic. It is well established that the ground shaking experienced at a given location depends on numerous factors beyond just magnitude, such as local site conditions, source mechanism, region, depth, and rupture directivity. Therefore, the existence and the reliability of the input data such as digital elevation model, geologic map, and ground-shaking parameters are also essential for a comprehensive analysis.

A few authors have started to develop models that take a more complete view of the driving factors (e.g., Kritikos et al., 2015; Marc, Hovius, & Meunier, 2016; Nowicki et al., 2014). However, the literature is still relatively sparse, in part because it is challenging and time consuming to pull together input data sets (e.g., EQIL inventories) that cover the wide range of conditions under which EQIL occurs. The importance of different tectonic, geomorphologic, and climatic settings to landslide distribution patterns and the internal relation between EQIL-related factors such as landslide number, size-frequency distribution, and total landslide-affected area still requires further investigation using EQIL inventories from many different environments.

Even though landslide susceptibility assessment using different statistical analyses has become a common approach, the use of seismic indicators in these analyses to estimate EQIL hazard is still rare (Budimir et al., 2014; Carro et al., 2003; Gallen et al., 2016; Lee, 2014; Marzorati et al., 2002; Nowicki et al., 2014; Robinson et al., 2017). The generation of EQIL hazard maps for new or scenario events is complicated as each earthquake has specific characteristics, and existing EQIL inventories only reflect the characteristics of a single earthquake. For statistical EQIL hazard assessments, many more EQIL inventories are needed to represent the response to different amounts of ground shaking and regional differences in landslide susceptibility. Physically based methods are not prone to the same limitations, but the existing models are still rather simple and focus mainly on shallow landslides by applying the widely used Newmark method (Jibson et al., 2000). Other models use weighted approaches that combine a number of factor maps but do not use information on frequency and expected landslide densities (e.g., Kritikos et al., 2015) or utilize statistical approaches that assume a single relationship between landslide occurrence and susceptibility to landsliding across the globe (e.g., Nowicki et al., 2014).

A limited number of preliminary studies have used EQIL inventories to produce globally applicable models for near real-time prediction of seismically induced landslides (Godt et al., 2008; Kritikos et al., 2015; Marc, Hovius, Meunier, Gorum et al., 2016; Nowicki et al., 2014). Though they are not yet sufficiently mature to operationally inform disaster response after earthquakes, the development of such models benefits greatly from the availability of past data for model development and testing. The more data available, the better the models can become.

Beyond its value for the hazard studies, having more EQIL data could also help us to improve our understanding in terms of some other natural processes such as erosion, sediment transportation, landscape evolution, and climatic and environmental change. For example, Malamud et al. (2004b) relate the magnitude of earthquakes to erosion rates using EQIL inventories. Parker et al. (2011) analyze the relationships between coseismic slip, mass wasting, and relief generation considering the landslides triggered by the Wenchuan earthquake. Marc, Hovius, Meunier, Gorum et al. (2016) use EQIL inventories to derive total landslide volumes and area affected. Later, Marc, Hovius, and Meunier (2016) use this knowledge to assess seismic mass-balance over multiple earthquakes. Gallen et al. (2015) suggest the EQIL inventories can be a useful tool to probe the near-surface environment for spatial patterns of material strength. On the other hand, Schlögel et al. (2011) try to detect climatic and environmental change by analyzing landslide inventories. Although the authors do not use particularly the EQIL inventories in their studies, having a larger EQIL database could also provide opportunity to increase the quality in such studies.

These findings emphasize the importance of collecting EQIL inventories from as many past events as possible and making them easily accessible to the EQIL community. We can use them to better understand the causal factors of the landslide distribution under different conditions, which can help determine landslide susceptibility, hazard, vulnerability, and risk, and can provide rapid assessments of landslide densities after an earthquake (Guzzetti et al., 2012). Though there are two national scale EQIL databases for Italy (Martino et al., 2014)

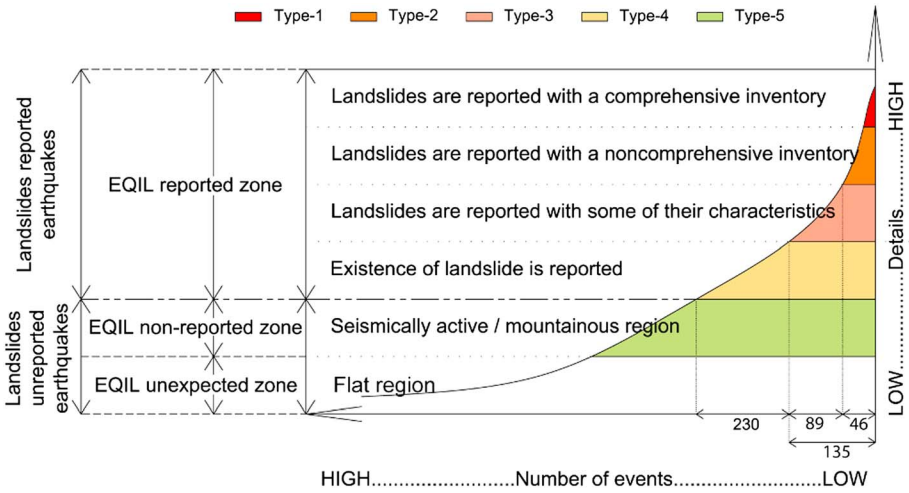

Figure 1. Schematic graph showing the different types of EQIL data sources. The numbers in the lower right corner refer to the number of EQIL events of each data type currently available to our knowledge.

and New Zealand (Rosser et al., 2017), currently no global-scale centralized database exists for recording these events and storing the available inventory maps.

In this work, we strive to overcome and account for some of these issues, which are mainly caused by the scarcity of data, in order to create an openly available EQIL database and promote progress in this field. We have compiled 66 digital EQIL inventories from numerous authors. We have created a centralized repository using the U.S. Geological Survey's ScienceBase platform for sharing the inventories that we have permission from the original authors to redistribute.

In the following sections, we present the results of our compilation. First, we summarize the EQIL data sources and define different data types to categorize them. Based on the available inventories, we analyze EQIL distributions for different years, continents, countries, and mountain belts. Frequency distributions are presented for some of the reported EQIL parameters such as total area affected, total number of landslides, landslide area, maximum distance from fault rupture and epicenter location, slope angle, ruggedness, local relief, distance to stream, peak ground acceleration (PGA), peak ground velocity (PGV), and Modified Mercalli Intensity (MMI). We conclude by establishing a schema for evaluating EQIL inventories utilizing published standards for ideal inventories (Harp et al., 2011; Xu, 2014), applying this to the EQIL inventories in our database, discussing implications for using EQIL inventories for a range of applications, and detailing the ScienceBase repository we created for openly sharing EQIL inventories with the community.

2. EQIL Data Types

Earthquake-induced landslide information is presented in the literature with large variability in detail and data format because they were generated by many different researchers with different methods, objectives, and priorities. For some earthquakes, there are comprehensive spatial landslide data available, whereas for other cases, we cannot even be sure whether a single landslide was triggered. For example, within 1 week of the main shock of 15 April 2016 in Kumamoto earthquake (M_w = 7), the Geospatial Information Authority of Japan provided a basic landslide inventory on their web site (http://www.gsi.go.jp/). This swift provision is attributed to efficient landslide interpretation and mapping using ortho-photos, produced by digital aerial photos, Global Navigation Satellite System and Inertial Measurement Unit measured aerial triangulation, and semi-automated mosaic image producing. On the other hand, for the earthquake of 7 December 2015 that occurred in mountainous region of Tajikistan (M_w = 7.2), no information on landslide occurrence is available. Because of gaps such as this, there are an unknown number of undocumented events in addition to the known EQIL events presented here.

Figure 1 illustrates how we can evaluate information obtained from different sources. The first major division separates earthquakes with or without reported landslides. Depending on this division, we have defined five types of data sources ranging from Type 1 to Type 5.

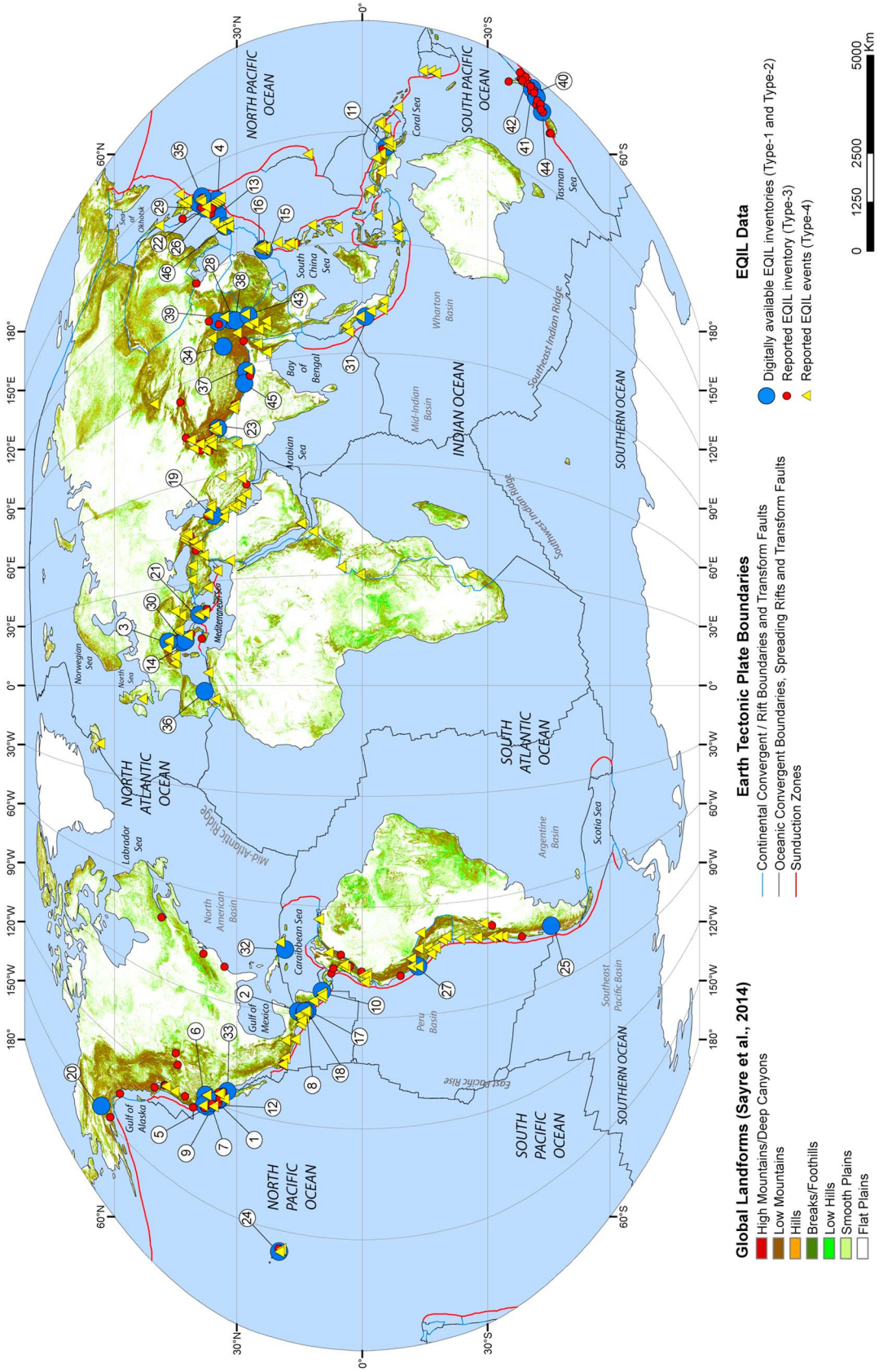

Figure 2. Location of EQIL reported events (with and without inventories; digitally available EQIL inventories are marked with same IDs listed in Table 1).

Landslide inventory maps are the most useful EQIL data source. Ideally, they contain records on the location, date of occurrence, and attribute information such as age, depth of failure, degree and style of activity, and landslide type for each mapped landslide (Guzzetti et al., 2000; Guzzetti et al., 2012; Hansen, 1984; McCalpin, 1984; Pašek, 1975; Wieczorek, 1984). However, to our knowledge, no EQIL inventory satisfies all these ideal conditions. In reality, ancillary information such as landslide size and (or) type can be presented at best in high-detail EQIL inventories. In this study, we have named these high-detail inventories data source Type 1 (Figure 1). However, such inventories are compiled for few earthquakes that trigger landslides, and we observe that many of the available inventories lack the relevant attribute information. We have named these low-detail inventories data source Type 2 (Figure 1).

In this study, we have collected either the digital or hardcopy versions of the inventories after contacting the authors or organizations producing the inventories. We have converted the hardcopy inventory maps to shape files that can be used in a GIS. As a result of these efforts, we were able to collect EQIL digital inventory maps for 46 earthquakes (Figure 2 and Table 1). For some earthquakes, multiple inventories are available from different sources; therefore, we have 64 digital EQIL inventories that can be classified as either Type-1 or 2-data. More EQIL inventories have been produced, but the originators of these data either did not respond, declined to share their inventories, or we did not know about them.

In several cases, the publications describing EQIL do not contain actual inventory maps, and only the general characteristics of the landslide distribution are given (Type-3 inventories). For example, Keefer (1984) used 40 EQIL inventories in his study. Although this is one of the few global-scale EQIL studies, only a limited number of inventory maps referred to in this study are accessible today. D. K. Keefer (written communication(s), 2016) indicated that EQIL inventory maps were only available for a few of the 40 reported earthquakes, and the general relations and conclusions reported were pieced together from various resources, listed in Keefer and Tannaci (1981). Information from the general characteristics of these events can still be significant, and thus we add the Type-3 events to our database. Because EQIL characteristics cannot be directly verified from an inventory, Type-3 events might introduce more uncertainty and outliers into the observations, and thus these data should be used with care. We carried out an extensive literature review of EQIL events and were able to find an additional 89 earthquakes having at least one reported EQIL inventory (Type 3 in Figure 1). We have extracted some landslide characteristics for these events, such as the approximate landslide-affected area, the total number of landslides, and the maximum landslide distance to the epicenter and rupture zone. Additionally, we listed fault types, earthquake magnitude, and focal depth for these events. The complete list is presented in Table S1 in the supporting information.

In addition to the above mentioned EQIL data types, for some earthquakes we only know of the existence of triggered landslides without any other information. For these events, we do not have reliable qualitative, quantitative, or spatial information on the triggered landslides. We have named this data source Type 4 (Figure 1). Marano et al. (2010) compiled such events in their study; they used the catalogue of the U.S. Geological Survey's Prompt Assessment of Global Earthquakes for Response (PAGER) system, PAGERCAT (Allen et al., 2009). This database was compiled from news reports and official sources available at the time of publishing. Based on this catalogue, 276 earthquakes from 1968 to 2008 had confirmed EQIL occurrences, of which 51 overlap with events classified as Type 3, Type 2, or Type 1. Therefore, the database from Marano et al. (2010) contributes 225 additional landslide-triggering earthquakes (Figure 2), giving a total of 363 reported EQIL events.

It is also useful to collect data on null events (earthquakes in mountainous environments that did not trigger landslides) in order to understand the causes and mechanisms of EQIL. If no landslides are reported for a particular earthquake, it may be that the earthquake did not cause any landslides, or that it did but the landslides were not documented. We classify these as Type 5 (Figure 1). However, no official recording procedure exists for earthquakes that do not trigger landslides. Therefore, identifying null events with certainty is not possible.

3. Analysis of EQIL Characteristics

In what follows, we review the characteristics of the EQIL events presented in this database, discussing general aspects of each inventory; important characteristics to consider before utilizing these data are discussed, including specific features of EQIL inventories of Type 1 and Type 2.

AGU Journal of Geophysical Research: Earth Surface

10.1002/2017JF004236

Table 1
List of the Digitally Available EQIL Inventories (as of September 2016)

ID	Location	Date /time	Epicenter location	Data type	Magnitude	Depth (km)	Number of landslides	Total landslide area (km^2)	Fault type	Reference study
1	San Fernando, California (USA)[a]	1971-02-09 /14:00:41 UTC	34.416°N 118.370°W	Pt	6.6 (M_w)	8.9	391	N/A	S	Morton (1971)
2	Guatemala	1976-02-04/09:01:43 UTC	15.324°N 89.101°W	Plg	7.5 (M_w)	5.0	6,224	60.8	S	Harp et al. (1981)
3	Friuli (Italy)	1976-05-06/20:00:11 UTC	46.356°N 13.275°E	Plg/Pt	6.5 (M_s)	9.0	1,007	1.1	T	Govi (1977)
4	Izu Oshima Kinkai (Japan)	1978-01-14/03:24:39 UTC	34.809°N 139.259°E	Plg	6.6 (M_s)	14.0	659	1.5	S	Suziki (1979)
5	Mount Diablo, California (USA)	1980-01-24/19:00:09 UTC	37.852°N 121.815°W	Pt	5.8 (M_w)	11.0	105	N/A	S	Wilson et al. (1985)
6	Mammoth Lakes, California (USA)[a]	1980-05-25/19:44:50 UTC	37.696°N 118.750°W	Plg	6.5 (ML)	6.0	4,027	33.8	NDC	Harp et al. (1984)
7	Coalinga, California (USA)	1983-05-02/23:42:37 UTC	36.240°N 120.300°W	Plg	6.7 (ML)	9.6	3,980	4.8	T	Harp and Keefer (1990)
8	San Salvador (El Salvador)	1986-10-10/17:49:24 UTC	13.827°N 89.118°W	Pt	5.7 (M_w)	7.0	268	N/A	S	Rymer (1987)
9a	Loma Prieta, California (USA)	1989-10-18/00:04:15 UTC	37.036°N	Pt	6.9 (Mh)	17.2	1775	N/A	T	Keefer and Manson (1998)
9b	Loma Prieta, California (USA)		121.880°W	Plg			138	0.4	T	McCrink (2001)
10	Limon (Costa Rica)	1991-04-22/21:56:51 UTC	9.685°N 83.073°W	Plg	7.6 (M_w)	10.0	1,643	8.2	T	Marc, Hovius, and Meunier (2016)
11	Finisterre Mt./(Papua N. G.)[a]	1993-10-13/02:06:00 UTC	5.889°S 146.020°E	Plg	6.9 (M_w)	25.3	4,790	69.0	T	Meunier et al. (2008)
12	Northridge, California (USA)	1994-01-17/12:30:55 UTC	34.213°N 118.537°W	Plg	6.7 (M_w)	18.2	11,111	23.8	T	Harp and Jibson (1995)
13	Hyogo-ken Nanbu (Japan)	1995-01-16/20:46:52 UTC	34.583°N 135.018°E	Plg	6.9 (M_w)	21.9	2,353	0.5	S	Uchida et al. (2004)
14a	Umbria-Marche (Italy)[a]	1997-09-26/09:40:26 UTC	43.084°N	Pt	6.0 (M_w)	10.0	233	N/A	N	Esposito et al. (2000) and Antonini et al. (2002)
14b	Umbria-Marche (Italy)[a]		12.812°E	Plg			210	1.9		Marzorati et al. (2002)
15	Jueili (Taiwan)	1998-07-17/04:51:14 UTC	23.407°N 120.736°E	Plg	5.7 (M_w)	12.6	847	4.8	T	Huang and Lee (1999)
16	Chi-Chi (Taiwan)	1999-09-20/17:47:18 UTC	23.772°N 120.982°E	Plg	7.7 (M_w)	33.0	9,272	127.5	T	Liao and Lee (2000)
17	Santa Tecla (El Salvador)	2001-01-13/17:33:32 UTC	13.049°N 88.660°W	Pt	7.7 (M_w)	60.0	139	N/A	N	Ministerio de Medio Ambiente y Recursos Naturales, El Salvador (2001)
18	Santa Tecla (El Salvador)	2001-02-13/14:22:05 UTC	13.671°N 88.938°W	Pt	6.6 (M_w)	10.0	62	N/A	S	
19	Avaj (Iran)	2002-06-22/02:58:21 UTC	35.626°N 49.047°E	Pt	6.5 (M_w)	10.0	50	N/A	T	Mahdavifar et al. (2006)
20	Denali Alaska (USA)	2002-11-03/22:12:41 UTC	63.517°N 147.444°W	Plg	7.9 (M_w)	4.9	1,579	121.2	S	Gorum et al. (2014)
21	Lefkada Ionian Islands (Greece)	2003-08-14/05:14:54 UTC	39.160°N 20.605°E	Plg	6.3 (M_w)	10.0	274	2.9	S	Papathanassiou et al. (2013)
22a	Mid-Niigata (Japan)[a]	2004-10-23/08:56:00 UTC	37.226°N	Plg	6.6 (M_w)	16.0	10,516	14.4	T	GSI of Japan (2005)
22b	Mid-Niigata (Japan)[a]		138.779°E	Plg			4,615	12.6		Sekiguchi and Sato (2006)
22c	Mid-Niigata (Japan)[a]			Plg			3,922	8.1		Yagi et al. (2007)
23a	Kashmir (India-Pakistan)	2005-10-08/03:50:40 UTC	34.539°N	Plg	7.6 (M_w)	26.0	2,424	10.4	T	Sato et al. (2007)
23b	Kashmir (India-Pakistan)		73.588°E	Plg			1,461	49.9		Basharat et al. (2014)
23c	Kashmir (India-Pakistan)			Plg			2,930	109.4		Basharat et al. (2016)
24	Kiholo Bay (Hawaii)	2006-10-15/17:07:49 UTC	19.878°N 155.935°W	Plg	6.7 (M_w)	38.9	383	2.8	N	Harp et al. (2014)
25a	Aysen Fjord (Chile)[a]	2007-04-21/17:53:46 UTC	45.243°S	Plg	6.2 (M_w)	36.7	540	17.2	S	Sepúlveda et al. (2010)
25b	Aysen Fjord (Chile)[a]		72.648°W	Plg			517	13.2	S	Gorum et al. (2014)
26a	Niigata Chuetsu-Oki (Japan)	2007-07-16/01:13:22 UTC	37.535°N	Plg	6.6 (M_w)	12.0	312	0.4	T	Kokusai Kogyo (2007)
26b	Niigata Chuetsu-Oki (Japan)		138.446°E	Pt			70	N/A		Collins et al. (2012)

Journal of Geophysical Research: Earth Surface

10.1002/2017JF004236

Table 1. *(continued)*

ID	Location	Date /time	Epicenter location	Data type	Magnitude	Depth (km)	Number of landslides	Total landslide area (km^2)	Fault type	Reference study
27	Pisco/(Peru)	2007-08-15/23:40:57 UTC	13.386°S 76.603°W	Plg	8.0 (M_w)	39.0	271	1.1	T	Lacroix et al. (2013)
28a	Wenchuan (China)	2008-05-12/06:28:01 UTC	31.002°N	Pt	7.9 (M_w)	19.0	13,114	N/A	T	Qi et al. (2010)
28b	Wenchuan (China)		103.322°E	Plg			59,108	812.2		Dai et al. (2011)
28c	Wenchuan (China)			Pt			60,109	N/A		Gorum et al. (2011)
28d	Wenchuan (China)			Plg			197,481	1159.9		Xu, Xu, Yao et al. (2014)
28e	Wenchuan (China)			Plg			69,605	530.3		Li et al. (2014)
28f	Wenchuan (China)			Plg			6,727	54.6		Tang et al. (2016)
29	Iwate-Miyagi Nairiku (Japan)	2008-06-13/23:43:45 UTC	39.030°N 140.881°E	Plg	6.9 (M_w)	7.8	4,211	14.4	T	Yagi et al. (2009)
30a	L'Aquila/Abruzzo (Italy)[a]	2009-04-06/01:32:39 UTC	42.334°N	Pt	6.3 (M_w)	8.8	570	N/A	N	Guzzetti et al. (2009)
30b	L'Aquila/Abruzzo (Italy)[a]		13.334°E	Pt			89	N/A		Piacentini et al. (2013)
31	Sumatra (Indonesia)	2009-09-30/10:16:09 UTC	0.720°S 99.867°E	Pt	7.6 (M_w)	81.0	87	N/A	T	Umar et al. (2014)
32a	Haiti	2010-01-12/21:53:10 UTC	18.443°N	Plg	7.0 (M_w)	13.0	4,490	7.98	S	Gorum et al. (2013)
32b	Haiti		72.571°W	Plg			23,567	24.85		Harp et al. (2016)
33	Sierra Cucapah (Mexico)	2010-04-04/22:40:42 UTC	32.286°N 115.295°W	Plg	7.2 (M_w)	10.0	453	0.7	S	Barlow et al. (2014)
34	Yushu (China)	2010-04-13/23:49:38 UTC	33.165°N 96.548°E	Plg	6.9 (M_w)	17.0	2,036	1.2	S	Xu et al. (2013)
35	Eastern Honshu (Japan)	2011-03-11/05:46:24 UTC	38.297°N 142.373°E	Plg	9.1 (M_w)	29.0	3,475	4.35	T	Wartman et al. (2013)
36	Lorca (Spain)	2011-05-11/16:47:25 UTC	37.699°N 1.672°W	Pt	5.1 (M_w)	1.0	270	N/A	S	Alfaro et al. (2012)
37	Sikkim (India)	2011-09-18/12:40:51 UTC	27.730°N 88.155°E	Pt	6.9 (M_w)	50.0	164	N/A	S	Chakraborty et al. (2011)
38a	Lushan (China)	2013-04-20/00:02:47 UTC	30.308°N	Plg	6.6 (M_w)	14.0	1,289	5.2	T	Li et al. (2013)
38b	Lushan (China)		102.888°E	Pt			15,546	18.5		Xu et al. (2015)
39	Minxian-Zhangxian (China)	2013-07-21/23:45:56 UTC	34.512°N 104.262°E	Plg	5.9 (M_w)	8.0	2,330	0.8	T	Xu, Xu, Shyu et al. (2014)
40	Cook Straight (New Zealand)	2013-07-21/05:09:31 UTC	41.704°S 174.337°E	Pt	6.5 (M_w)	17.0	35	N/A	S	Van Dissen et al. (2013)
41	Lake Grassmere (New Zealand)	2013-08-16/02:31:05 UTC	41.734°S 174.152°E	Pt	6.5 (M_w)	8.2	501	N/A	S	Van Dissen et al. (2013)
42	Eketahuna (New Zealand)	2014-01-20/02:52:44 UTC	40.660°S 175.814°E	Pt	6.1 (M_w)	28.0	176	N/A	N	Rosser et al. (2014)
43	Ludian (China)	2014-08-03/08:30:13 UTC	27.189°N 103.409°E	Plg	6.2 (M_w)	12.0	1,024	5.2	S	Ying-ying et al. (2015)
44	Wilberforce (New Zealand)	2015-01-05/17:48:42 UTC	43.055°S 171.236°E	Pt	5.6 (M_w)	8.1	265	N/A	S	GNS Science (2015)
45a	Gorkha (Nepal)	2015-04-25 06:11:25 UTC	28.231°N	Pt	7.8 (M_w)	8.2	4,312	N/A	T	Kargel et al. (2016)
45b	Gorkha (Nepal)[a]		84.731°E	Plg			2,654	15.6		Zhang et al. (2016)
45c	Gorkha (Nepal)			Plg			2,513	14.2		H. Tanyas, University of Twente, unpublished data, 2015
45d	Gorkha (Nepal)			Plg			24,903	86.5		Roback et al. (2017)
46a	Kumamoto (Japan)	2016-04-15/16:25:06 UTC	32.791°N	Plg	7.0 (M_w)	10.0	336	1.8	S	DSPR-KU (2016)
46b	Kumamoto (Japan)		130.754°E	Plg			2,742	8.2		NIED (2016)

Note. Inventories having the same number (e.g., 6a and 6b) relate to the same earthquake.
[a]Landslides that can be attributed to more than one earthquake (M_w: Moment magnitude; M_s: Surface-wave magnitude; ML: Local magnitude; Plg: Polygon; Pt: Point; S: Strike-slip fault; T: Thrust fault; N: Normal fault; NDC: Nondouble couple earthquake).

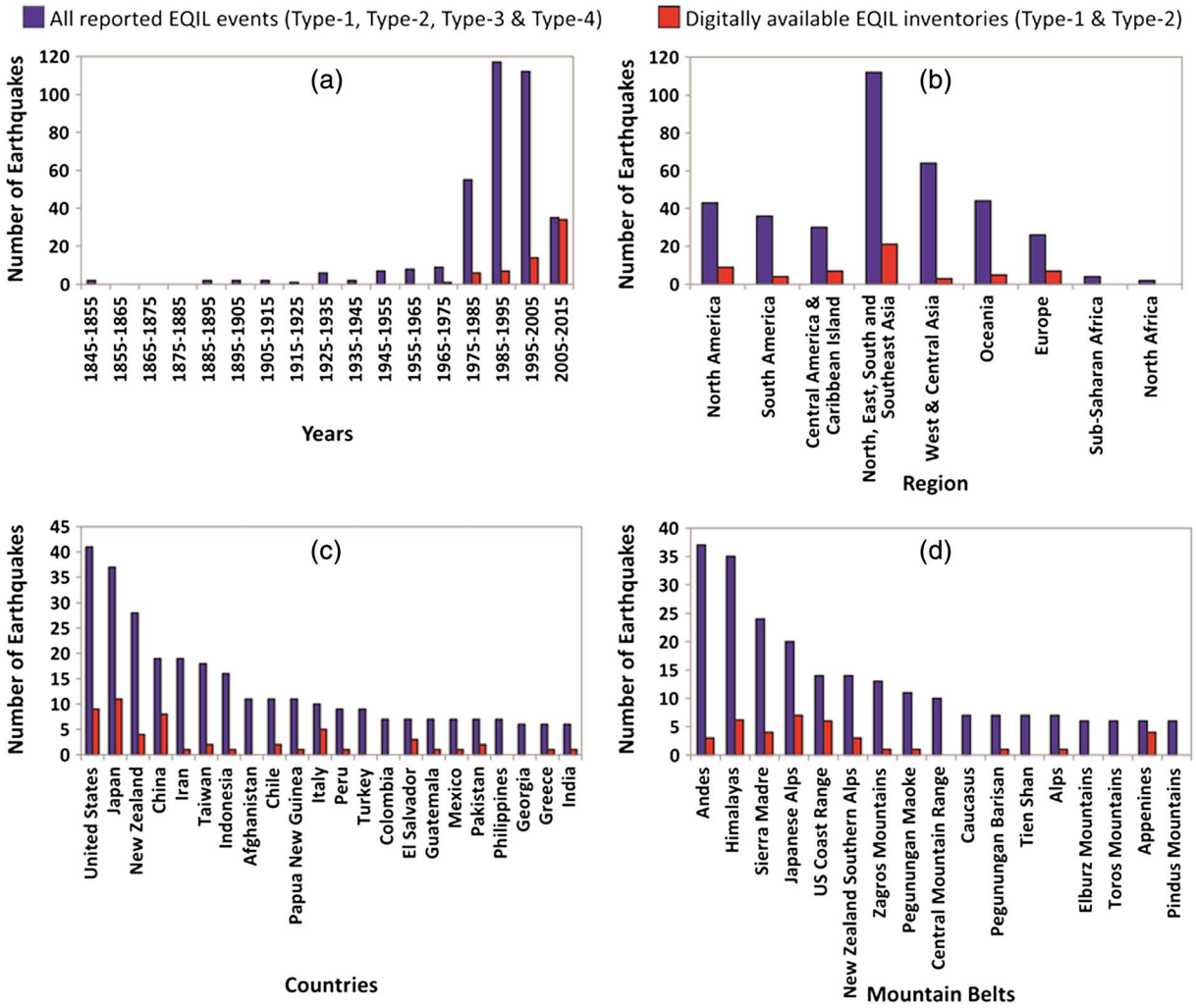

Figure 3. Number of reported EQIL events and digitally available EQIL inventories shown by (a) 10 year period, (b) region, (c) country, and (d) mountain belt.

3.1. Analysis of Reported EQIL Events

Although our database of 363 reported EQIL events includes events as early as the 1840s, more than 85% of the known events were documented after 1975 (Figure 3a). Since that time, innovations in data acquisition systems and remote sensing techniques have led to a sharp increase in the quantity of reported EQIL events and digitally available inventories. Because the data provided from the PAGER system only covers 1968–2008, and we divide the data into 10 year intervals, an artificial decrease is shown in the number of reported events occurring after 2005 (Figure 3a). Work is ongoing to continue the PAGER-related work for the period from 2008 until present.

Overall, only 10% of reported EQIL events have available digital inventories. About 90% of the reported EQIL events are from America, Oceania, and Asia. Only a few inventories are available for Europe, and none exist for Africa (Figure 3b and Table 2). About half of the inventories come from the USA, Japan, New Zealand, China, Iran, Taiwan, and Indonesia (Figure 3c and Table 2). For both Iran and Indonesia, only one digital inventory is available, although almost 20 EQIL events were reported for each.

From a morphological point of view, about 80% of all reported events and inventories belong to major mountain belts (Figure 3d and Table 2), such as the Andes, Himalayas, Sierra Madre, Japanese Alps, U.S. Coast Range, New Zealand Southern Alps, and Zagros Mountains.

Table 2
Number of EQIL Reported Events by Country, Region, and Mountain Belt

Country	# of Inv/# of Eqs[a]	Region (# of Inv/# of Eqs[a])	Mountain Belt	# of Inv/# of Eqs[a]
Canada	0/2	North America (9/44)	Alaska Range	1/3
			Appalachian Mountains	0/3
			Cascade Range	0/5
			Coastal Mountains	0/1
United States	9/42		Coast Range	6/15
			Rocky Mountains	0/2
			Sierra Nevada	1/3
Argentina	0/2	South America (3/36)	Andes	3/37
Bolivia	0/1			
Chile	2/11			
Colombia	0/7			
Ecuador	0/5			
Peru	1/9			
Venezuela	0/1			
Costa Rica	1/5	Central America and Caribbean Island (8/30)	Sierra Madre	4/24
Dominican Rep.	0/1			
El Salvador	3/7			
Guatemala	1/7			
Haiti	2/1			
Mexico	1/7			
Nicaragua	0/1			
Panama	0/1			
Bangladesh	0/1	North, East, South, and Southeast Asia (29/113)	Alishan Range	2/3
			Altay Mountains	0/3
China	10/19		Caucasus	0/7
			Central Mountain Range	0/10
India	1/6		Cordillera Central	0/4
			Dalou Mountains	3/3
Indonesia	1/16		Himalayas	8/35
			Japanese Alps	7/20
Japan	11/37		Kunlan Shan	0/2
Myanmar	0/1		Qinling Mountains	1/3
Nepal	5/4		Pegunungan Barisan	1/7
Philippines	0/7		Xueshan Range	0/5
Russia	0/3		Sierra Madre	0/1
Taiwan	2/18		Tien Shan	0/7
Afghanistan	0/11	West and Central Asia (3/64)	Eastern Black Sea Mountains	0/4
Armenia	0/1			
Cyprus	0/1		Elburz Mountains	0/6
Georgia	0/6			
Iran	1/19		Sulaiman Range	0/1
Kyrgyzstan	0/1			
Pakistan	3/7		Tiamat Ash Shan	0/2
Palestine	0/1			
Tajikistan	0/5		Toros Mountains	0/6
Turkey	0/9			
Uzbekistan	0/1		Zagros	1/13
Yemen	0/2			
Guam	0/1	Oceania (5/44)	Central Range (Pegunungan Maoke)	1/11
New Zealand	4/28			
Papua New Guinea	1/11			
Solomon Island	0/1		Southern Alps	3/14
Vanuatu	0/3			
Bosnia and Herzegovina	0/1	Europe (8/26)	Alps	1/7
Croatia	0/1			
France	0/1		Appenines	4/6
Greece	1/6			
Iceland	0/1		Cambrian Mountains	0/1
Italy	6/10			
Romania	0/1		Carpathian	0/1

Table 2. *(continued)*

Country	# of Inv/# of Eqs[a]	Region (# of Inv/# of Eqs[a])	Mountain Belt	# of Inv/# of Eqs[a]
Slovenia	0/2			
Serbia	0/1		Dinaric Alps	0/3
Spain	1/1		Pindus Mountains	0/6
United Kingdom	0/1		Vatnajökull	0/1
Algeria	0/1	North Africa (0/2)	Atlas Mountains	0/2
Morocco	0/1		Drakensberg	0/1
South Africa	0/1		Ethiopian Highlands	0/1
Sudan	0/1	Sub-Saharan Africa (0/4)	Kenyan Highlands	0/2
Uganda	0/1			

[a]Number of digitally available EQIL inventories/number of reported EQIL events.

3.2. Analysis of Reported EQIL Characteristics

Here we examined the relation between documented characteristic features of Type-1, Type-2, and Type-3 EQIL events (Figure 1) and four parameters that are reported for the majority of the events (Table S1): the approximate area affected by landslides, the total number of landslides, the maximum distance from the fault-rupture zone, and the epicentral distance. To calculate the approximate area affected by landslides, we defined a polygon including the all landslides for the analyzed inventory and calculate the area of that polygon. For the maximum distance measures, we took the farthest landslide and calculated its perpendicular distance to the fault-rupture zone and earthquake epicenter. To identify the fault-rupture zone, we used the fault trace if there is no surface rupture. For Type-1 and Type-2 events, we obtained the available fault plane/surface rupture and epicenter location from the literature.

Figure 4 shows the frequency distribution of the EQIL events for these parameters, without taking into account different levels of completeness. However, the level of completeness influences the total area

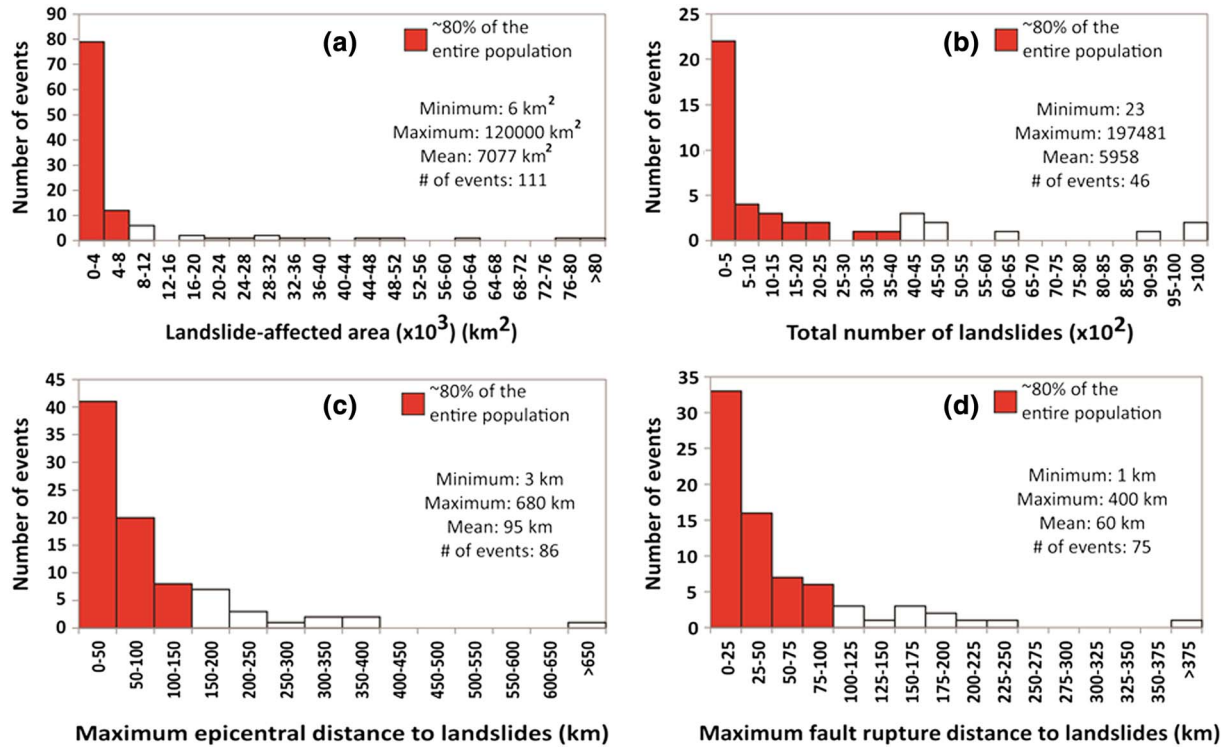

Figure 4. Frequency values and basic statistics for (a) the landslide-affected area, (b) the total number of landslides, (c) the maximum epicentral distance to landslides, and (d) the maximum fault-rupture distance to landslides. Red bars show the range of values for 80% of the total number of EQIL events in the database for which information was available. Since many inventories are not complete, in most cases, these refer to minimum values.

affected by landslides and the total number of landslides in a given inventory, so these numbers should be considered minimum values in most cases.

Although there is significant variability, more than 80% of the EQIL events affected areas (area containing all mapped landslides) less than 10,000 km^2; the maximum value is 120,000 km^2 for the Wenchuan event (Figure 4a). Likewise, for about 80% of the inventories, the total number of landslides is less than 4,000; however, about 200,000 landslides (Figure 4b) were triggered in the 2008 Wenchuan event (Xu, Xu, Yao et al., 2014). Additionally, for about 80% of the inventories, maximum distances to epicenter and fault-rupture zone are less than 150 km (Figure 4c) and 100 km (Figure 4d), respectively.

3.3. Analysis of Digital EQIL Inventories

Type-1 and Type-2 data provide means for detailed EQIL characterization. These data sources include 66 EQIL inventories from 46 earthquakes, and each has a varying level of quality and completeness. Landslides were delineated as polygon vector data for 44 of the available digital EQIL inventories; the other 22 were represented as points. To compare both types of inventories during this evaluation, we reduced each polygon to a single point by assigning a point at the highest elevation of each landslide polygon (as a proxy for the initial source point of the landslide). By doing so, we have 554,333 landslide-initiation points in this database; this landslide population is dominated by the Wenchuan earthquake because 406,144 of the landslides belong to six inventories for this event, which were made by five independent groups. The inventory of Xu, Xu, Yao et al. (2014) can be considered as an updated version of the Dai et al. (2011) inventory. Even this single Wenchuan inventory (Xu, Xu, Yao et al., 2014) contains approximately 76,000 more landslides than the total of all other inventories. The Wenchuan event was an extraordinary EQIL event where a large magnitude earthquake occurred along the steepest boundary of the Tibetan Plateau (Fielding, 1996; Liu-Zeng et al., 2011). The anomalously large number of landslides triggered by this event dominates the observations coming from different inventories. Joint evaluation of Wenchuan and other inventories can bias hazard upward. Therefore, we decided to evaluate these five Wenchuan inventories separately, excluding the Dai et al. (2011) inventory to avoid duplications.

The landslide points were analyzed first in terms of topographic factors including slope, local relief, distance to streams, and vector ruggedness measure (VRM). VRM is a terrain ruggedness measure that quantifies local variation in terrain more independently of slope than other methods such as land surface ruggedness index or terrain ruggedness index (Sappington et al., 2007). It is derived by incorporating the heterogeneity of both slope and aspect. The Shuttle Radar Topography Mission digital elevation model (about 30 m resolution) (NASA Jet Propulsion Laboratory, 2013) was used in the analyses. Frequency distributions for these parameters show that the highest landslide frequencies are concentrated in particular intervals for all of these parameters (Figure 5). Landslides related to the Wenchuan inventories show different distributions and mean values. When we look at the entire data set (excluding Wenchuan inventories), the mean values for slope, VRM, local relief, and the distance to streams are 27° (Figure 5a), 0.035 (Figure 5b), 524 m (Figure 5c), and 413 m (Figure 5d), respectively. However, for the Wenchuan inventories, the mean values for the same parameters are 35° (Figure 5e), 0.09 (Figure 5f), 916 m (Figure 5g), and 468 m (Figure 5h). Therefore, as explained earlier, we can have a better understanding of the general characteristics of EQIL if we exclude the Wenchuan event. By excluding Wenchuan, we can conclude that about 80% of the remaining population of EQIL occurs within the interval of 10–45° (Figure 5a), 0–0.05 (Figure 5b), 200–800 m (Figure 5c), and 0–700 m (Figure 5d) for slope, VRM, local relief, and distance to stream, respectively.

We investigated ground-shaking parameters in a similar manner. Estimated values of peak ground acceleration (PGA), peak ground velocity (PGV), and Modified Mercalli Intensity (MMI) were obtained at the location of each landslide from the U.S. Geological Survey (USGS) ShakeMap Atlas 2.0 (Garcia et al., 2012). As in the previous analysis, we discussed the Wenchuan inventories separately (Figure 6).

Contrary to what was found for the topographic parameters, the distributions and mean values for the seismic parameters are quite similar for the Wenchuan inventories and all others. For the inventories excluding Wenchuan, the mean PGA, PGV, and MMI values are 0.5 m/s^2 (Figure 6a), 47 cm/s (Figure 6b), and 7.3 (Figure 6c), and those for the three Wenchuan inventories are 0.6 m/s^2 (Figure 6d), 35 cm/s (Figure 6e), and 7.4 (Figure 6f). For the entire database excluding the Wenchuan event, approximately 80% of the

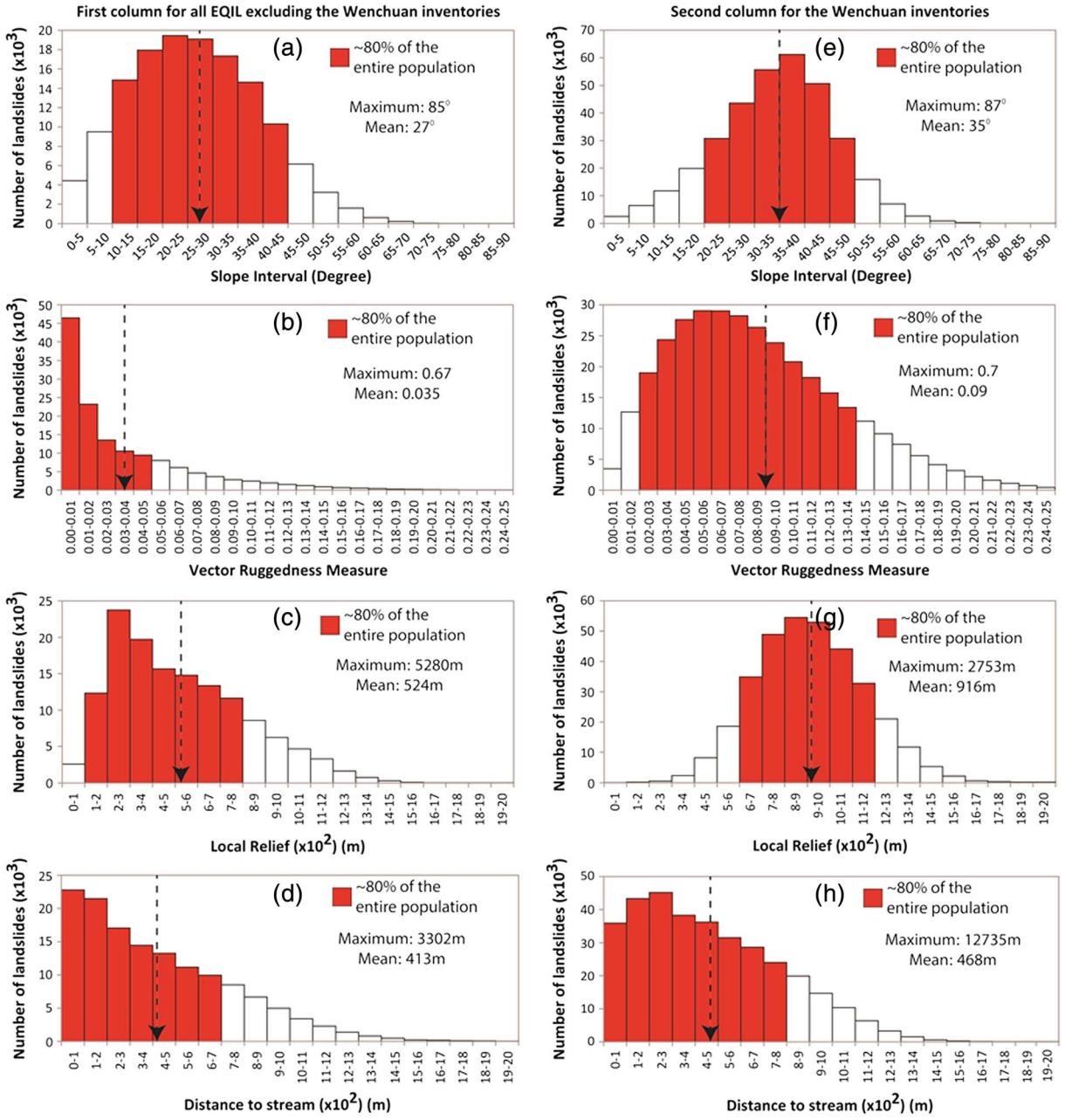

Figure 5. Frequency values of earthquake-induced landslides in intervals of (a) slope, (b) vector ruggedness measure (VRM), (c) local relief, and (d) distance to stream for all EQIL excluding the Wenchuan inventories (in first column), and for the (e–h) Wenchuan inventories separately (in second column). The arrows point out the mean values.

population of EQIL are observed in the interval for PGA of 0.1–0.8 m/s^2 (Figure 6a), for PGV of 0–70 cm/s (Figure 6b), and for MMI between 6.5 and 7.0 (Figure 6c).

We also analyzed the landslide-size distributions for the collected polygon-based landslide inventories in our database. Multiple studies have shown that the frequency-area distribution (FAD) of medium and large landslides follows a power law (e.g., Guzzetti et al., 2002; Malamud et al., 2004a) with a characteristic power law exponent. For most landslide inventories, noncumulative power law exponents occur in the range of 1.4–3.4, with a central tendency of 2.3–2.5 (Stark & Guzzetti, 2009; Van Den Eeckhaut et al., 2007). We calculated the power law exponents for 43 inventories in our database based on the method proposed by Clauset et al., (2009) and analyzed the number of inventories for the obtained power law exponent intervals (Figure 7a).

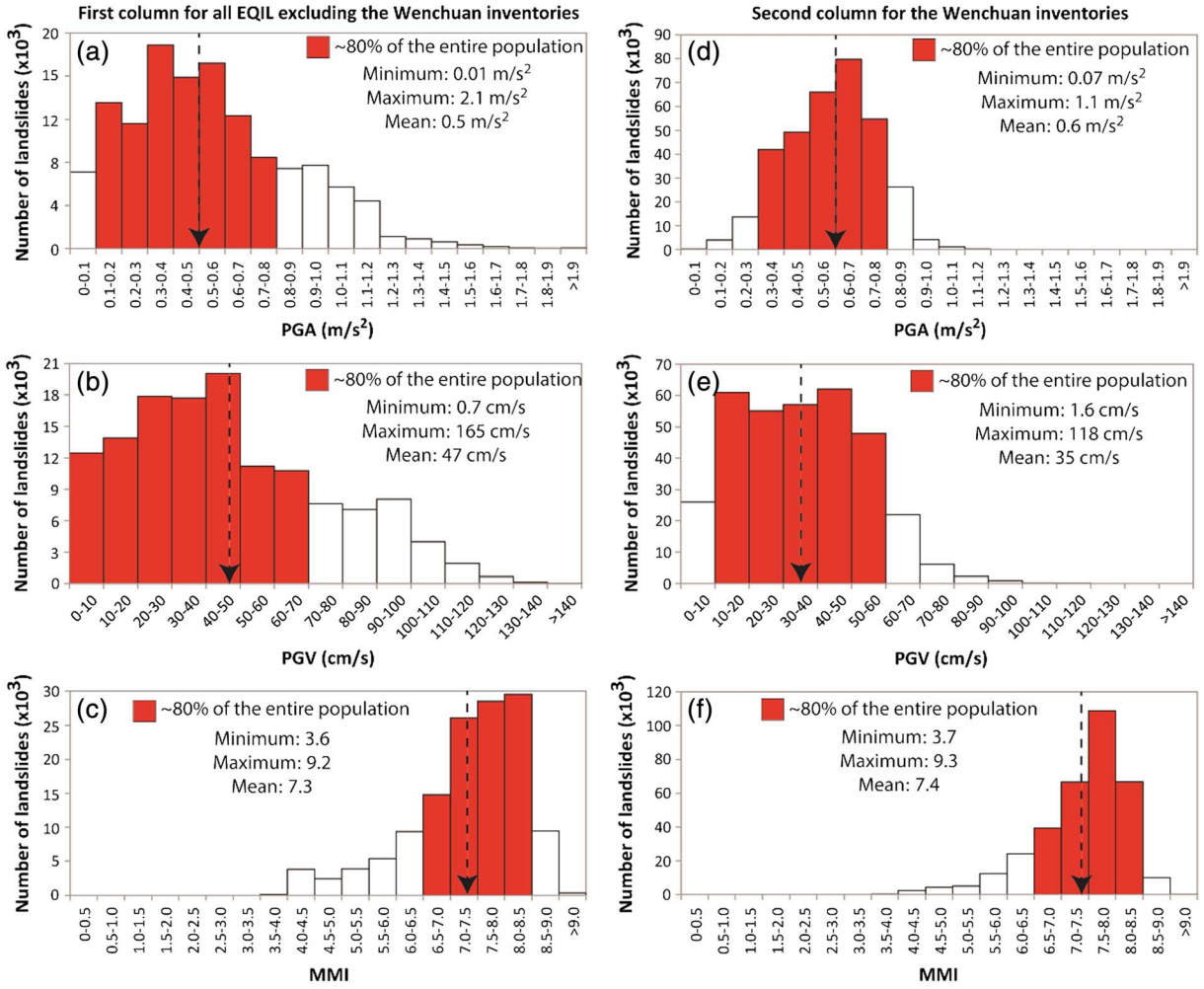

Figure 6. Frequency values of earthquake-induced landslides in intervals of (a) PGA, (b) PGV, and (c) MMI for all EQIL excluding the Wenchuan inventories (in first column) and for the (d–f) Wenchuan inventories separately (in second column). The arrows point out the mean values.

The results showed that the mean exponent value is 2.5, consistent with findings cited above. Due to the high population of medium-sized landslides, the two polygon-based Wenchuan inventories (Li et al., 2014; Xu, Xu, Yao et al., 2014) yield the highest power law exponent values, which are 3.1 and 3.2. This could be caused by a large number of amalgamated smaller landslides that increase the frequency of medium-sized landslides. We also visually analyzed the range of landslide sizes in the EQIL inventories by combining all landslide polygon areas from the inventories (separating the Wenchuan inventories from the others) and plotting the FADs (Figure 7b). Similar to the FADs of the individual EQIL inventories, FADs of the combined inventories follow the power law distribution, with power law exponent of 3.3 for the Wenchuan inventories and 2.3 for the combination of all other inventories, which included 43 inventories provided by different groups using different mapping techniques (Figure 7b). Mapped landslides range from a few square meters to a few million square meters in area. The smaller landslides constitute the majority of the database. For the Wenchuan inventories, 80% of all landslides are smaller than 8,000 m^2, whereas, for the other inventories, 80% of the landslides are smaller than 4,000 m^2. The rollover point (most commonly mapped landslide size) is about 1,000 m^2 for the Wenchuan inventories but only around 100 m^2 for the combined FAD of the other inventories. Also, the rollover in the Wenchuan inventories is relatively sharper in comparison with the combined FAD of the other inventories. These differences are possibly caused by the mapping procedure of landslides—so many landslides were triggered by Wenchuan earthquake, that it was not practical to map the small ones completely.

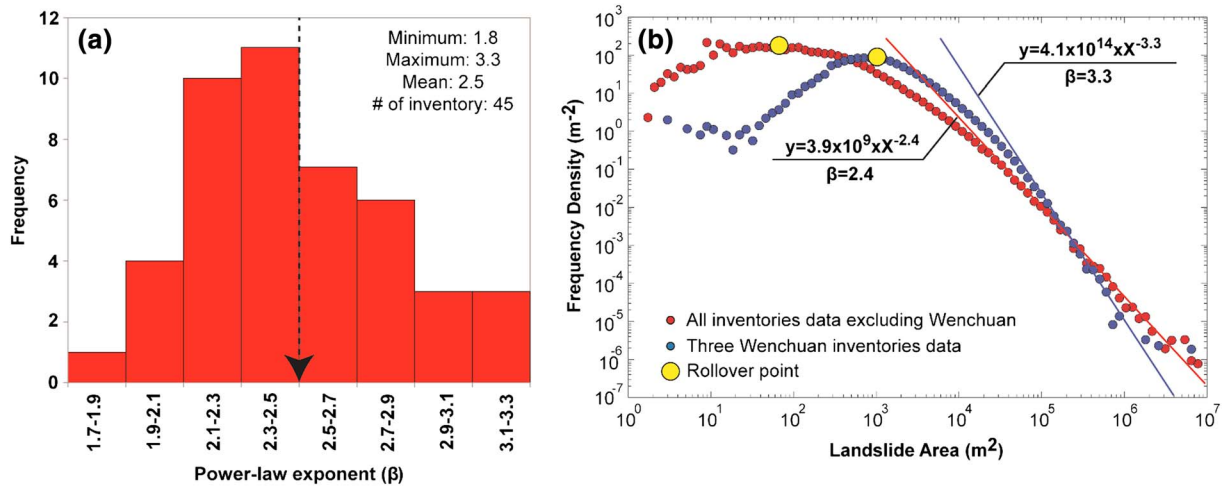

Figure 7. (a) Frequencies for estimated power law exponents for the EQIL inventories and (b) the frequency-density distributions for the landslides gathered from all inventories excluding the Wenchuan event (red) and the landslides gathered from the two Wenchuan inventories (blue). The arrow points out the mean value.

4. Evaluation of EQIL Inventories

A limited number of digital EQIL inventories are available worldwide, and the available ones differ greatly in quality, completeness, and representation. Therefore, establishing guidelines and adequate metadata for future inventories is essential (Wasowski et al., 2011).

Several studies analyzed the quality and completeness of landslide inventories using a number of criteria (Gorum, 2013; Harp et al., 2011; Keefer, 2002; Wasowski et al., 2011). Harp et al. (2011) defined three basic criteria for evaluating inventories: (1) coverage of the entire area affected by landslides, (2) inclusion of all landslides down to a small enough scale, and (3) depiction of landslides as polygons rather than points. They listed 10 inventories that satisfied these criteria and thus can be considered comprehensive: 1976 Guatemala (M = 7.5) (Harp et al., 1981), 1978 Izu Oshima KinKai (M = 6.6) (Suziki, 1979), 1980 Mammoth Lakes (M = 6.5) (Harp et al., 1984), 1983 Coalinga (M = 6.3) (Harp & Keefer, 1990), 1993 Hakkaido Nansei-oki (M = 7.8) (Tanaka, 1994), 1994 Northridge (M = 6.7) (Harp & Jibson, 1995), 1995 Hyogoken Nanbu (M = 6.9) (Nishida et al., 1996), 1999 Chi-Chi (M = 7.7) (Liao & Lee, 2000), 2004 Mid-Niigata (M = 6.6), (GSI, 2005; Sekiguchi & Sato, 2006; Yagi et al., 2007), and 2008 Iwate-Miyagi-Nairiku (M = 6.9) (Yagi et al., 2009) earthquakes.

We have only eight of these inventories (Guatemala, Izu Oshima KinKai, Mammoth Lakes, Coalinga, Northridge, Chi-Chi, Mid-Niigata, and Iwate-Miyagi-Nairiku) reported by Harp et al. (2011). Therefore, the majority of the EQIL inventories do not meet these criteria. For a robust statistical analysis, however, we need to maximize the number of inventories used. This creates a trade-off between quality and completeness. The 2007 Niigata Chuetsu-Oki (Japan) event is a good example to illustrate this. Three inventories are available for this event. The first inventory (Collins et al., 2012) used a combination of field observations and analysis of oblique aerial photos for a relatively small area. During the detailed field investigation, preearthquake landslides were eliminated, and 70 EQIL were mapped as point data. The second study (Kokusai Kogyo, 2007) was carried out using only 1/6,000 aerial photo interpretation covering about 400 km^2 in area and resulted in 312 landslides mapped as polygons. In the third inventory (Sato et al., 2008), 1/10,000 aerial photos covering about 260 km^2 in area were used for image interpretation followed by field verification, which resulted in 172 landslides mapped. These three inventories were prepared following partly the same method but yielded quite different inventory maps, both in representation and in the number of landslides mapped.

A much more striking example is the 2008 Wenchuan (China) EQIL inventories. Xu, Xu, Yao et al. (2014) compared four inventory maps that they classified as nearly complete and reported significant differences in the number of landslides mapped. In those studies, about 196,000, 59,000, 60,000, and 11,300 landslides were mapped by Xu, Xu, Yao et al. (2014), Dai et al. (2011), Gorum et al. (2011), and Huang and Li (2009), respectively. The number of landslides in two inventories called "nearly complete" prepared for the same event

differs by a factor of about 17. As a consequence, although all inventories contain valuable information, the use of these in our analysis would yield contrasting results. Therefore, we need a methodology to evaluate the comprehensiveness of inventories to provide a basis for selecting which inventories to include in a given analysis. By combining the evaluation of quality, completeness, and representation, we can picture the comprehensiveness of any inventory.

The quality of any EQIL inventory can be defined based on its accuracy, which is the geographical and thematic correctness of the information shown on the map (Guzzetti et al., 2012). To evaluate the quality of EQIL inventory, ideally we could address the following questions: (i) Were the landslides mapped at the right location? (ii) Were the landslides mapped using a comprehensive mapping methodology? (iii) Were the landslides mapped by experienced people? (iv) Were the landslides types classified with a consistent classification method (e.g., Keefer, 1984)? (v) Were the results of individual landslide mappers crosschecked by others? (vi) How much total time did producer(s) spend on the landslide inventory map? (vii) Were contiguous landslides mapped separately or as a single landslide? (viii) How long after the earthquake was the inventory completed? (ix) Were problematic areas field checked after creating the inventory? (x) Was the boundary of mapped area indicated?Completeness measures the extent to which an EQIL inventory includes all coseismic landslides for a specific earthquake (Guzzetti et al., 2012). To evaluate the completeness of EQIL inventory, we need to address the following questions: (i) Were the landslides mapped for the entire landslide-affected area or only for a part of the area? (ii) Was a minimum size threshold used for mapping landslides? (iii) Were preearthquake and postearthquake landslides removed from the inventory?

Evaluating an EQIL inventory based on these criteria is complicated because many of them, especially the quality evaluation criteria, cannot be evaluated. For example, evaluating the landslide interpretation skills of the mapper, the detail of the mapping, and whether coalescing landslides are mapped separately or as a single polygon are difficult to evaluate without going back and examining the original imagery. Therefore, any evaluation regarding the quality and completeness of EQIL inventories has some limitations.

Quality and completeness of an inventory are two different terms that do not have to be met for the same inventory. For instance, a high-quality EQIL inventory can be incomplete if the inventory is provided partially, or a complete inventory can be low quality if landslides are not located, differentiated, or classified appropriately. Beyond that, to evaluate the comprehensiveness of the inventory, there is another component: representation.

The methods of evaluating how well an inventory represents reality will be different depending on the representation type. For a point-based inventory, under ideal conditions, the point should be assigned to a consistent and clearly defined part of the landslide, ideally the scarp. Furthermore, we would expect to have the type and size of landslides in the attribute table. For a polygon-based inventory, we would expect to have an inventory with different landslide types, and differentiated source and depositional areas.

We have developed an evaluation methodology to provide a basis for selecting which inventories to include in a given analysis. To accomplish this task, we have defined a mixed set of criteria that we can evaluate without having detailed metadata of each inventory. We have used eight criteria (Table 3) that are partly derived from earlier studies (Gorum et al., 2011; Harp et al., 2011; Xu, 2014). The criteria defined for the evaluation of EQIL inventories are described in the following sections.

4.1. Evaluation Criteria

The methodology used for generating an EQIL inventory is very important for the overall evaluation of the inventory. Guzzetti et al. (2012) categorized the different methods used to prepare landslide inventories into four groups: (a) (semi) automated satellite image classification; (b) observations based on aerial reconnaissance (helicopter flights, fixed-wing aircraft or UAVs (Unmanned Aerial Vehicles); (c) field survey, and (d) visual image interpretation (using satellite images or aerial photography).

If preearthquake and postearthquake images are utilized, (semi) automated image classification techniques can be the most effective approach, especially because they provide rapid results (e.g., Lacroix et al., 2013; Martha et al., 2010). However, these methods are still not capable of identifying coalescing landslides or landslides that are mostly vegetated, and they cannot classify landslides by type. Moreover, automated techniques are prone to errors due to misidentification of features such as bare-earth slopes, recent fills, rock quarries, road cuts, and other excavations as landslides.

Table 3
Evaluation Scheme for EQIL Inventories, Using Two Sets of Criteria, With Score

Category					
(A)	(B)		Criteria	Execution performance	Score
Essential criteria	Essential criteria	(i)	Was the study area analyzed systematically by visual interpretation?	0–100%	0–1
		(ii)	Was the boundary of the mapped area indicated?	No/Yes	0/1
		(iii)	Were the preearthquake and postearthquake landslides eliminated from the inventory?	0–100%	0–1
		(iv)	Was the mapping resolution of inventory enough to differentiate the individual landslides? (L = Linear resolution of rollover point)	$L > 25$ m: <0.5 25 m $\geq L > 5$ m: ≥ 0.5 5 m $\geq L$: 1	0/1
Preferred criteria		(v)	Were the landslides mapped as polygons?	No/Yes	0/1
		(vi)	Did landslide polygons differentiate source and depositional areas?	No/Yes	0/1
	Preferred criteria	(vii)	Were the landslides field checked in problematic areas?	0–100%	0–1
		(viii)	Were the landslides classified according to type?	No/Yes	0/1

As another alternative method, aerial reconnaissance, either by fixed-wing aircraft, helicopter, or UAV, might provide detailed information for specific areas but cannot cover the entire affected area. Field mapping of landslides (Brunsden, 1985) allows characterization of landslide features such as type, depth, source, and depositional area, which might not be obtainable by any other methodology. Nevertheless, mapping landslides in the field is hampered by difficulties of landslide detection because it is not straightforward to identify the boundary of landslides, especially if they are large (Guzzetti et al., 2012). Moreover, this method is limited by the time and resources available and the accessibility of the area.

Utilization of the multiple approaches to get the most information possible within monetary and time constraints could be the idealized method for EQIL mapping. On the other hand, if you evaluate the methods individually, of all available methods, visual image interpretation leads to the best results, because expert interpreters can omit nonlandslide features and can systematically scan the whole affected area as long as cloud-free imagery is available. If high-resolution imagery is available, landslides can be classified by type, and source and depositional areas can be identified. Visual image interpretation can be carried out for the entire landslide-affected area or for specific sample areas to support and validate other methods such as (semi) automatic image classification.

To analyze the conditions that cause landslide initiation, both the presence and absence of landslides are important information that should be obtained from the inventories. Harp et al. (2011) stress the importance of indicating the boundaries of the mapped landslide area. Due to limitations in the available images, resources, time, and cloud cover, mapping of the whole region affected by landslides might not be possible, but as long as the boundary of the mapped area is defined, it can still be valuable information. If the inventories do not indicate the mapping boundaries, but the extent of the utilized satellite imagery or flight lines of aerial surveys are indicated, such boundaries can still be defined. Based on this approach, the availability of a mapping boundary can be evaluated.

Removing landslides that occurred before and after the earthquake is essential to provide an accurate inventory of triggered features. For example, the 2015 Gorkha earthquake in Nepal occurred in a mountainous area that is highly susceptible to rainfall-induced landslides; thus, if the preearthquake landslides are not eliminated from the inventory, many landslides not caused by this earthquake could be erroneously related to the seismic triggering event. Therefore, the imagery must be acquired as soon as possible after the earthquake to capture the initial aspects of the landslides and the terrain (Harp et al., 2011). Several approaches can be used to remove preearthquake landslides from the inventory, including through information gathered from local people (e.g., Chakraborty et al., 2011), field observations (e.g., Harp & Jibson, 1995; Harp & Keefer, 1990), or the use of preevent and postevent imagery (e.g., Barlow et al., 2014; Papathanassiou et al., 2013; Xu, Xu, Yao et al., 2014). The last method is considered the best option.

Harp et al. (2011) stated that an ideal inventory should include all detectable landslides down to sizes of 1–5 m in length. However, it is difficult to determine the completeness of the mapping of such small features. The minimum landslide size observed in an inventory is generally not representative of the resolution of

inventories because such small landslides might be mapped only for a limited part of inventories where the imagery is of the highest quality.

Malamud et al. (2004a) suggest a functional definition of completeness that requires a landslide inventory to include a substantial fraction of all landslides at all scales. In this definition, the rollover point refers to the most commonly occurring landslide size in the inventory. Parker et al. (2015) take the position of rollover as the minimum size where landslide mapping is complete. Based on this approach, we evaluated the rollover points of the inventories. If the linear resolution of the rollover point is less than 5 m, we assumed that the inventory satisfies the ideal conditions in terms of mapping resolution, and if it is higher than 25 m, we assumed that it is far from the ideal conditions. A caveat is that the rollover position may also be controlled by the mechanical properties of the substrate (Frattini & Crosta, 2013; Stark & Guzzetti, 2009), and therefore, some inventories may not be "incomplete" but only occur in place where the mechanics do not allow small landslides ($<$5 m) very often.

Since, the rollover point is not only related to the resolution of utilized imagery but also the mapping technique, this evaluation is not enough to be sure whether the mapped landslides are well delineated or not. Furthermore, except for the producer of the inventory, it is difficult for anyone to evaluate how successfully the individual landslides were mapped. There is a methodology (Marc & Hovius, 2015) proposed for the automatic detection of amalgamated polygons, and it works based on geometric and topographic considerations. In this EQIL inventory database, we have five inventories that were corrected based on the referring method by Marc, Hovius, and Meunier (2016): 2007 Aysen Fjord (Gorum et al., 2014), 1999 Chi-Chi (Liao & Lee, 2000), 1976 Guatemala (Harp et al., 1981), 1994 Northridge (Harp & Jibson, 1995), and 2008 Wenchuan (Dai et al., 2011) EQIL inventories. However, the methodology provides only a partial correction for amalgamated landslides. Along the same slope, multiple landslides can be triggered and amalgamated. For such cases, the suggested methodology is not capable of detecting amalgamation. Therefore, through the aforementioned mapping resolution evaluation, we can only reach a conclusion about whether the completely mapped minimum landslide size of inventory is enough to differentiate the individual landslides. Beyond this evaluation, any user who works on mobilized landslide masses or frequency-area statistics of landslides should give special attention to amalgamated landslides.

Having landslides mapped as polygons rather than points is important to evaluate the overall area of landslides related to a given earthquake and to estimate the mobilized total volume of material using empirical relations relating landslide area and volume (e.g., Klar et al., 2011; Larsen et al., 2010). Moreover, the source and depositional areas of landslides can be represented only with a polygon-based inventory. Therefore, it is preferred to delineate landslides as polygons (Harp et al., 2011).

While it is preferable to delineate landslides as polygons, it is even better to separate landslide source and depositional areas into separate polygons (Gorum et al., 2013); landslides mapped this way provide a basic demarcation of landslide processes, and only the conditions in the source area are relevant for the analysis of causal factors. For example, in terms of slope steepness at the landslide source we typically find much steeper slopes than in the depositional area. Also, it is important to separate source and depositional areas in order to calculate the runout distance and the total mobilized mass volume triggered by an earthquake. The lack of differentiation of source and depositional parts of landslides is one of the most significant sources of uncertainty in all landslide frequency-size related discussions. Despite the importance of this information, there are only two EQIL inventories (the 2004 Mid-Niigata by GSI of Japan, 2004 and the 2015 Gorkha by Roback et al., 2017) in our database that separated source and deposition areas. On the other hand, estimating source areas from polygon inventories is possible; Jibson et al. (2000) mapped landslides as single polygons and then used the upper half of those polygons as the assumed source area.

Field surveying is not generally the optimal method to produce a landslide inventory map because it is time consuming and often impossible to cover the entire affected area. However, it is still necessary for validating any inventory map prepared using other techniques (Guzzetti et al., 2012). With the advances in remote sensing techniques (related to very high resolution images and UAVs), the emphasis on field surveys has decreased. Field surveying for validation is suggested only for a limited part of the inventory area, generally less than 15% (Galli et al., 2008), or for verifying specific problematic areas that are difficult to identify from satellite imagery (Guzzetti et al., 2012).

Keefer (1984) evaluated EQIL by considering the type of material, landslide movement, degree of internal disruption of the landslide mass, and geologic environment and classified them into three main types of landslides. Different landslide types have different combinations of causal factors (Crosta et al., 2012). Nevertheless, few EQIL inventories include landslide types (e.g., 1989 Loma Prieta (M = 6.9) by Keefer, 2002; 1997 Umbria-Marche (M = 6.0) and 2009 Abruzzo by Guzzetti et al., 2009; 2011 Lorca (M = 5.1) by Alfaro et al., 2012; and 2011 Eastern Honshu (M = 9.1) by Wartman et al., 2013).

In addition to the details of EQIL inventories, Table 4 also includes the relative quality grading of each ShakeMap as developed by Wald et al., (2008). This grading scale allows users to evaluate the relative uncertainty level of each ShakeMap for postearthquake or historical earthquake ShakeMap analyses (Wald et al., 2008). In this grading system, meant primarily for the quick evaluation of near-real-time maps, uncertainty levels of ShakeMaps are presented by letters from "A" to "F," based on high- to poor-quality constraints, respectively. Lower grades are typically assigned to larger ($M > 6$) events for which there are few stations and the fault rupture area is not available. Higher grades are typically given to ShakeMaps with numerous seismic stations and/or intensity observations, and for which the fault dimensions are constrained. For landslide analyses, those ShakeMaps with higher grades can thus be considered more reliable than those with lower grades. However, often the data constraints used to compute these grades are from reported or assigned intensities, and the summary grades do not necessarily address whether or not there were seismic recordings in the areas where landslides occurred. Thus, in principle, since each ShakeMap has spatially varying uncertainty estimates, site-specific uncertainty values should be used to consider the reliability of shaking at landslide sites.

4.2. Evaluating EQIL Inventories Using the Criteria

Making an overall evaluation of the inventories using a single score ignores the fact that each of the inventories was created for a different purpose. Furthermore, the available information about inventories is not enough to make an accurate quality or completeness evaluation. Therefore, instead of such an evaluation, we separated the proposed criteria into two groups of essential and preferred criteria (Table 3). The essential criteria can be considered as the minimum criteria for any application of the EQIL inventory to work. The preferred criteria can be considered as the criteria we prefer for most EQIL-related applications, but they are not as significant as the essential criteria.

The content of the essential and preferred criteria can show variety based on the scope of the study. For instance, in landslide susceptibility and hazard studies, the mapping unit does not have to be represented by a polygon. Similarly, differentiations between the source and depositional areas or landslide types are not necessarily available for every landslide susceptibility or hazard study. In this case, the mentioned criteria can be considered as preferred criteria instead of essential. Likewise, for landslide risk assessments, if authors do not consider the runout behavior of landslides, they do not really need the landslide polygons or source versus depositional area to be differentiated. However, this information might also be required for specific hazard analyses that focus on particular landslide size range or landslide type. On the other hand, if authors focus on landform evaluation caused by EQIL, the mobilized landslide mass volume/area would be important, and in that case source and depositional areas of landslide polygons would be essential. Therefore, we considered several purposes of landslide-inventory applications (Guzzetti et al., 2012) and defined two categories for EQIL inventory-related applications: (1) inventories to make a landslide susceptibility or hazard assessment, or to investigate the distribution, types, and patterns of landslides in relation to morphological and geological characteristics, and (2) inventories to study evolution of landscapes dominated by mass-wasting processes (landslide dynamic and erosion studies). For each category, we defined sets of different essential and preferred criteria (Table 3). The user can check these essential criteria to complete an overall evaluation of which inventories are appropriate for their application of the data. Also, they can take a particular set of criteria into account for a specific application and evaluate the available inventories.

Table 4 presents the results of applying the criteria described above to each of the EQIL inventories in the database. Each EQIL inventory is evaluated with a score between 0 and 1 for each criterion, some of which are binary (Table 3). If the criterion is fully satisfied, then the score is one; if the criterion is fully ignored, then it is zero. Intermediate values between zero and one indicate that the criterion is partially satisfied. To make an overall evaluation on each criterion, if the score is equal or greater than 0.5 for a criterion, we assume that the criterion is satisfied.

Table 4
Summary Chart for the Evaluation of EQIL Inventories and Uncertainty of Shakemaps for the Corresponding Events

		Criteria								
ID	Inventories	(i)	(ii)	(iii)	(iv)	(v)	(vi)	(vii)	(viii)	Quality of Shakemap (grade)
1	San Fernando	✓						✓		A
2	Guatemala	✓	✓	✓	✓	✓		✓		B
3	Friuli	✓	✓			✓			✓	A
4	Izu Oshima Kinkai	✓	✓	✓	✓	✓	✓	✓		C
5	Mount Diablo							✓		A
6	Mammoth Lakes	✓	✓	✓		✓		✓		A
7	Coalinga	✓	✓	✓	✓	✓		✓		A
8	San Salvador	✓		✓				✓		C
9a	Loma Prieta	✓	✓					✓		A
9b	Loma Prieta	✓	✓		✓	✓		✓		
10	Limon	✓	✓	✓		✓				B
11	Finisterre	✓	✓	✓		✓				N/A
12	Northridge	✓	✓	✓	✓	✓		✓		A
13	Hyogo-ken Nanbu	✓	✓	✓	✓	✓		✓		A
14a	Umbria-Marche	✓	✓	✓				✓	✓	A
14b	Umbria-Marche	✓	✓			✓		✓	✓	
15	Jueili	✓	✓	✓		✓				C
16	Chi-Chi	✓		✓	✓	✓		✓		A
17	Santa Tecla									B
18	Santa Tecla									A
19	Avaj		✓					✓		A
20	Denali	✓	✓	✓		✓				B
21	Lefkada	✓	✓			✓		✓		A
22a	Mid-Niigata	✓	✓	✓	✓	✓	✓	✓		A
22b	Mid-Niigata	✓	✓	✓	✓	✓	✓	✓	✓	
22c	Mid-Niigata	✓	✓	✓	✓	✓	✓	✓	✓	
23a	Kashmir	✓	✓	✓	✓	✓		✓		A
23b	Kashmir	✓	✓			✓		✓		
23c	Kashmir	✓	✓			✓		✓		
24	Kiholo Bay	✓	✓		✓	✓				A
25a	Aysen Fjord	✓	✓	✓		✓		✓	✓	N/A
25b	Aysen Fjord	✓	✓	✓		✓				
26a	Niigata Chuetsu-Oki	✓	✓		✓	✓				A
26b	Niigata Chuetsu-Oki	✓	✓					✓		
27	Pisco	✓	✓	✓				✓		A
28a	Wenchuan	✓	✓					✓		A
28b	Wenchuan	✓	✓			✓		✓		
28c	Wenchuan	✓	✓	✓				✓		
28d	Wenchuan	✓	✓	✓		✓		✓		
28e	Wenchuan	✓	✓	✓		✓				
28f	Wenchuan	✓	✓	✓	✓	✓		✓		
29	Iwate–Miyagi Nairiku	✓	✓	✓	✓	✓		✓	✓	A
30a	L'Aquila/Abruzzo	✓						✓		A
30b	L'Aquila/Abruzzo	✓	✓	✓				✓	✓	
31	Sumatra	✓						✓		C
32a	Haiti	✓	✓	✓	✓	✓				A
32b	Haiti	✓	✓	✓	✓	✓		✓		
33	Sierra Cucapah	✓	✓	✓	✓	✓				A
34	Yushu	✓	✓	✓	✓	✓		✓		C
35	Eastern Honshu	✓	✓	✓	✓	✓		✓	✓	A
36	Lorca	✓						✓	✓	A
37	Sikkim							✓	✓	N/A
38a	Lushan	✓	✓		✓	✓		✓		C
38b	Lushan	✓	✓	✓	✓	✓				
39	Minxian-Zhangxian	✓	✓	✓	✓	✓				C
40	Cook Straight	✓						✓		A
41	Lake Grassmere	✓						✓		C
42	Eketahuna	✓						✓		A
43	Ludian	✓	✓	✓	✓	✓				C
44	Wilberforce	✓						✓		C
45a	Gorkha	✓	✓	✓				✓		C
45b	Gorkha	✓	✓	✓		✓		✓		
45c	Gorkha	✓	✓	✓	✓	✓				
45d	Gorkha	✓	✓	✓	✓	✓	✓	✓		
46a	Kumamoto	✓	✓		✓	✓				A
46b	Kumamoto	✓	✓		✓	✓				

Some inventories lacked the information needed to determine the score of the individual criteria. If an analyzed criterion is not addressed in the referred study, we assumed that it was not satisfied. For instance, in some cases the specific attribute information, which was mentioned in the referred paper, did not exist in the available digital inventory. In these cases, we evaluated the inventory based on the available data. The evaluation results for the individual criteria for all EQIL inventories in the database are given in Table 4, and scores are given in Table S2 in the supporting information.

It is important to note that some EQIL inventories in the database represent landslides triggered by an earthquake sequence rather than a main shock. For example, the 1993 Finisterre Mountains (Papua New Guinea) landslide inventory contains 5,000 landslides that were triggered by two earthquakes having magnitudes of M_w 6.7 and 6.9 (Meunier et al., 2008); the inventory does not distinguish which landslides were triggered by which earthquake. Such inventories are indicated as footnote a in Table 1.

5. Discussion

We compiled information on 363 earthquakes that triggered landslides; this includes 46 events for which 66 digital inventories were generated, 89 events for which some landslide characteristics were reported, and 230 events for which triggered landslides are known. We contacted individual researchers and organizations and asked them to share their data with us to compile this database.Many additional inventories have been compiled that were not included in this analysis either because we could not contact the authors, or we did not get their permission to use their inventory. Other inventories may also exist that are not published in international literature or are in non-English language journals or gray-literature reports. In the future, we anticipate that the number of digital EQIL inventories will increase substantially, paralleling advances in remote-sensing data and techniques, particularly the use of semi-automated image classification from high-resolution satellite images and the use of UAVs. However, guidelines are needed for the generation of EQIL inventories that take into account the quality, completeness, and representation criteria outlined in this study. Therefore, further studies are necessary in order to prepare such guidelines, and to bring together scientists to share their inventories in a common platform. When inventories are generated according to such guidelines, the criteria for evaluating their quality, completeness, and representation might also differ from the ones we proposed here for existing inventories. A recommended standard practice could include the following:

(i) Generate inventories through semi-automatic image classification.
(ii) Use preearthquake and postearthquake images to isolate landslides triggered by the earthquake.
(iii) Perform a quality check through visual image interpretation and field checking.
(iv) Map landslides as polygons and separate the source and depositional areas.
(v) Classify landslides according to type and style of movement.

The scoring system we suggest can be helpful in evaluating the suitability of EQIL inventories for a variety of applications. However, its utility is limited by the lack of knowledge regarding the analyzed EQIL inventories. The scoring system does not evaluate whether landslides are mapped correctly, how well the inventory is registered to a given coordinate system, or whether landslides are correctly classified. These are important aspects of a quality assessment but are much more difficult to evaluate without access to independent data. One solution is to make the satellite or aerial imagery used to generate the landslide inventory available so that others can examine the quality of the mapping. Developing a metadata description procedure for EQIL inventories that takes into account such criteria will also provide all users with a uniform way to evaluate the inventories.

The current paucity of publicly available EQIL data limits the range of scientific questions that can be addressed and impedes improvements in hazard assessments. One way to remove barriers to progress is to make the data easier for the community to access by collecting and share digital EQIL inventories through a centralized clearing house. To address this need, we have created a ScienceBase Community titled "An Open Repository of Earthquake-triggered Ground Failure Inventories" dedicated to making EQIL and liquefaction inventories openly available to the community (Schmitt et al., 2017). ScienceBase (www.sciencebase.gov) is a collaborative scientific data and information management platform developed by the USGS. Community pages are designated project spaces that can be expanded over time to include more data sets.

Our aim is to enable the contribution and sharing of published EQIL inventories and accompanying methodological details based on the guidelines and criteria presented in section 4 of this paper. The EQIL community and the general public will then have access to the inventories in the system, and they can be used for research and other applications. Researchers that generate EQIL maps will be able to submit their inventories for inclusion as they become available. By centralizing data access and making methodological details available, we anticipate that the platform will lead toward the development of inventory mapping best practices and will ease visualization and analysis of the data with reference to other geospatial data such as climate, lithology, and topography. It would also provide means to meet data availability requirements imposed by funding agencies and publishers. In the future, the existing ScienceBase Community could be used as the data source for the development of interactive tools, for example, presenting summary statistics and visualizations of landslide size, number, geographic extent, and earthquake parameters of one or many inventories. Qualitative and quantitative improvement of the data contained in the clearing house will also enable the development and delivery of near-real-time estimates of EQIL impacts driven by near-real-time earthquake products such as the USGS ShakeMap, PAGER, and ShakeCast. Such estimates, as proposed by Nowicki et al. (2014), would provide situational awareness to government agencies, aid agencies, the media, and the general public. Next steps toward such a system require expanded data sharing and metadata documentation.

6. Summary

The aim of this study was to catalogue the available information on EQIL data, assess their relative quality and limitations, and review the characteristics of EQIL events, both broadly and with reference to individual inventories. We discussed the quality, completeness, and representation of EQIL inventories and proposed a scoring method for an overall evaluation of EQIL inventories. We suggest that expanding current data-sharing practice is essential to make breakthroughs in our understanding regarding earthquake-induced landslides, and critical for the reduction of future societal losses.

Acknowledgments

For the sharing of their EQIL inventories, the authors are very grateful to following researchers: Brian D. Collins, Chenxiao Tang, Chong Xu, Chyi-Tyi Lee, Edwin L. Harp, F. C. Dai, Fausto Guzzetti, M. J. García-Rodríguez, Gen Li, George Papathanassiou, Geospatial Information Authority of Japan, Hiroshi Yagi, Jianqiang Zhang, John Barlow, Jose Delgado, Joseph Wartman, LI Wei-le, Masahiro Chigira, Mattia De Amicis, Muhammad Basharat, Pascal Lacroix, Saibal Ghosh, Sergio A. Sepúlveda, Shengwen Qi, Tai-Phoon Huang, Taro Uchida, Timothy P. McCrink, Tommaso Piacentini, and Tsuyoshi Wakatsuki. Thank you to Yoko Tamura (PASCO) for assistance with obtaining the data set provided by PASCO Corporation and Kokusai Kogyo Company Ltd of Japan and Sally Dellow (GNS Science) and Toko Takayama (Asia Air Survey Co., Ltd of Japan) for assistance with obtaining the data sets provided by GNS Science and National Institute for Land and Infrastructure Management of Japan. We would also like to thank Mario Reyes of the El Salvador Landslides Monitoring Center (Ministry of Environment and Natural Resources) for his assistance in providing landslide inventories from El Salvador, the Japan Landslide Society for providing the earthquake-induced landslide inventory, Kristin D. Marano for providing global records of earthquake-induced landslides, and David Wald, Michael Hamburger, and two anonymous reviewers for their comments and contributions. T. G. wishes to thank the Turkish Academy of Sciences for their support within the framework of the Distinguished Young Scientist Award Program (TÜBA-GEBIP). Any use of trade, firm, or product names is for descriptive purposes only and does not imply endorsement by the U.S. Government. The authors have no conflicts of interest related to the work reported in this paper. Data that we have permission to share are available through the ScienceBase Community, which is a collaborative scientific data and information management platform developed by the USGS.

References

Alfaro, P., Delgado, J., García-Tortosa, F., Lenti, L., López, J., López-Casado, C., & Martino, S. (2012). Widespread landslides induced by the M_w 5.1 earthquake of 11 May 2011 in Lorca, SE Spain. *Engineering Geology*, *137*, 40–52. https://doi.org/10.1016/j.enggeo.2012.04.002

Allen, T. I., Marano, K. D., Earle, P. S., & Wald, D. J. (2009). PAGER-CAT: A composite earthquake catalog for calibrating global fatality models. *Seismological Research Letters*, *80*(1), 57–62.

Antonini, G., Ardizzone, F., Cardinali, M., Galli, M., Guzzetti, F., & Reichenbach, P. (2002). Surface deposits and landslide inventory map of the area affected by the 1997 Umbria-Marche earthquakes. *Bollettino della Societa Geologica Italiana*, *121*(1), 843–853.

Barlow, J., Barisin, I., Rosser, N., Petley, D., Densmore, A., & Wright, T. (2014). Seismically-induced mass movements and volumetric fluxes resulting from the 2010 M_w = 7.2 earthquake in the Sierra Cucapah, Mexico. *Geomorphology*, *230*, 138–145. https://doi.org/10.1016/j.geomorph.2014.11.012

Basharat, M., Ali, A., Jadoon, I. A., & Rohn, J. (2016). Using PCA in evaluating event-controlling attributes of landsliding in the 2005 Kashmir earthquake region, NW Himalayas, Pakistan. *Natural Hazards*, *81*(3), 1999–2017. https://doi.org/10.1007/s11069-016-2172-9

Basharat, M., Rohn, J., Baig, M. S., & Khan, M. R. (2014). Spatial distribution analysis of mass movements triggered by the 2005 Kashmir earthquake in the Northeast Himalayas of Pakistan. *Geomorphology*, *206*, 203–214. https://doi.org/10.1016/j.geomorph.2013.09.025

Bird, J. F., & Bommer, J. J. (2004). Earthquake losses due to ground failure. *Engineering Geology*, *75*(2), 147–179. https://doi.org/10.1016/j.enggeo.2004.05.006

Brunsden, D. (1985). Landslide types, mechanisms, recognition, identification. Paper presented at landslides in the South Wales coalfield, edited by: Morgan, CS, Proceedings Symposium, April.

Budimir, M. E. A., Atkinson, P. M., & Lewis, H. G. (2014). Seismically induced landslide hazard and exposure modelling in Southern California based on the 1994 Northridge, California earthquake event. *Landslides*, *12*(5), 895–910. https://doi.org/10.1007/s10346-014-0531-8

Carro, M., De Amicis, M., Luzi, L., & Marzorati, S. (2003). The application of predictive modeling techniques to landslides induced by earthquakes: The case study of the 26 September 1997 Umbria–Marche earthquake (Italy). *Engineering Geology*, *69*(1–2), 139–159. https://doi.org/10.1016/s0013-7952(02)00277-6

Chakraborty, I., Ghosh, S., Bhattacharya, D., & Bora, A. (2011). Earthquake induced landslides in the Sikkim-Darjeeling Himalayas—An aftermath of the 18th September 2011 Sikkim earthquake (8 p.). Koltaka: Report of Geological Survey of India.

Clauset, A., Shalizi, C. R., & Newman, M. E. (2009). Power-law distributions in empirical data. *SIAM Review*, *51*(4), 661–703. https://doi.org/10.1137/070710111

Collins, B. D., Kayen, R., & Tanaka, Y. (2012). Spatial distribution of landslides triggered from the 2007 Niigata Chuetsu–Oki Japan earthquake. *Engineering Geology*, *127*, 14–26. https://doi.org/10.1016/j.enggeo.2011.12.010

Crosta, G., Agliardi, F., Frattini, P., & Sosoi, R. (2012). SafeLand deliverable 1.1: Landslide triggering mechanisms in Europe—Overview and state of the art (378 pp.). SafeLand FP7, Deliverable 1.1. Retrieved from https://www.ngi.no/download/file/5969

Dai, F., Xu, C., Yao, X., Xu, L., Tu, X., & Gong, Q. (2011). Spatial distribution of landslides triggered by the 2008 M_s 8.0 Wenchuan earthquake, China. *Journal of Asian Earth Sciences*, *40*(4), 883–895. https://doi.org/10.1016/j.jseaes.2010.04.010

DSPR-KU (2016). Slope movement condition by 2016 Kumaoto earthquake in Minami-Aso village (as of 19:00 JST on 18 Apr 2016) (in Japanese). Disaster Prevention Research Institute, Kyoto University. Retrieved from http://www.slope.dpri.kyoto-u.ac.jp/disaster_reports/2016KumamotoEq/2016KumamotoEq2.html

Esposito, E., Porfido, S., Simonelli, A. L., Mastrolorenzo, G., & Iaccarino, G. (2000). Landslides and other surface effects induced by the 1997 Umbria–Marche seismic sequence. *Engineering Geology*, *58*(3), 353–376. https://doi.org/10.1016/S0013-7952(00)00035-1

Fielding, E. J. (1996). Tibet uplift and erosion. *Tectonophysics*, *260*(1), 55–84. https://doi.org/10.1016/0040-1951(96)00076-5

Frattini, P., & Crosta, G. B. (2013). The role of material properties and landscape morphology on landslide size distributions. *Earth and Planetary Science Letters*, *361*, 310–319. https://doi.org/10.1016/j.epsl.2012.10.029

Gallen, S. F., Clark, M. K., & Godt, J. W. (2015). Coseismic landslides reveal near-surface rock strength in a high relief, tectonically active setting. *Geology*, *43*, 11–14. https://doi.org/10.1130/g36080.1

Gallen, S. F., Clark, M. K., Godt, J. W., Roback, K., & Niemi, N. A. (2016). Application and evaluation of a rapid response earthquake-triggered landslide model to the 25 April 2015 M_w 7.8 Gorkha earthquake, Nepal. *Tectonophysics*. https://doi.org/10.1016/j.tecto.2016.10.031

Galli, M., Ardizzone, F., Cardinali, M., Guzzetti, F., & Reichenbach, P. (2008). Comparing landslide inventory maps. *Geomorphology*, *94*(3), 268–289. https://doi.org/10.1016/j.geomorph.2006.09.023

Garcia, D., Mah, R., Johnson, K., Hearne, M., Marano, K., Lin, K., … So, E. (2012). ShakeMap Atlas 2.0: An improved suite of recent historical earthquake ShakeMaps for global hazard analyses and loss model calibration, paper presented at World Conference on Earthquake Engineering.

Geospatial Information Authority of Japan (2005). 1:25,000 damage map of the Mid Niigata prefecture earthquake in 2004: 3 sheets.

GNS Science (2015). Wilberforce earthquake: Preliminary findings of the landslide and ground deformation rapid aerial reconnaissance survey, GNS Science Report.

Godt, J., Sener, B., Verdin, K., Wald, D., Earle, P., Harp, E., & Jibson, R. (2008). *Rapid assessment of earthquake-induced landsliding*. Paper presented at Proceedings of the First World Landslide Forum. Tokyo: United Nations University.

Gorum, T. (2013). Towards a better understanding of earthquake triggered landslides (Doctoral dissertation), University of Twente.

Gorum, T., Fan, X., van Westen, C. J., Huang, R. Q., Xu, Q., Tang, C., & Wang, G. (2011). Distribution pattern of earthquake-induced landslides triggered by the 12 May 2008 Wenchuan earthquake. *Geomorphology*, *133*(3), 152–167. https://doi.org/10.1016/j.geomorph.2010.12.030

Gorum, T., Korup, O., van Westen, C. J., van der Meijde, M., Xu, C., & van der Meer, F. D. (2014). Why so few? Landslides triggered by the 2002 Denali earthquake, Alaska. *Quaternary Science Reviews*, *95*, 80–94. https://doi.org/10.1016/j.quascirev.2014.04.032

Gorum, T., van Westen, C. J., Korup, O., van der Meijde, M., Fan, X., & van der Meer, F. D. (2013). Complex rupture mechanism and topography control symmetry of mass-wasting pattern, 2010 Haiti earthquake. *Geomorphology*, *184*, 127–138. https://doi.org/10.1016/j.geomorph.2012.11.027

Govi, M. (1977). Photo-interpretation and mapping of the landslides triggered by the Friuli earthquake (1976). *Bulletin of the International Association of Engineering Geology-Bulletin de l'Association Internationale de Géologie de l'Ingénieur*, *15*(1), 67–72. https://doi.org/10.1007/BF02592650

Guzzetti, F., Cardinali, M., Reichenbach, P., & Carrara, A. (2000). Comparing landslide maps: A case study in the upper Tiber River basin, central Italy. *Environmental Management*, *25*(3), 247–263. https://doi.org/10.1007/s002679910020

Guzzetti, F., Malamud, B. D., Turcotte, D. L., & Reichenbach, P. (2002). Power-law correlations of landslide areas in central Italy. *Earth and Planetary Science Letters*, *195*(3), 169–183. https://doi.org/10.1016/S0012-821X(01)00589-1

Guzzetti, F., Mondini, A. C., Cardinali, M., Fiorucci, F., Santangelo, M., & Chang, K. -T. (2012). Landslide inventory maps: New tools for an old problem. *Earth-Science Reviews*, *112*(1), 42–66. https://doi.org/10.1016/j.earscirev.2012.02.001

Guzzetti, F., Esposito, E., Calducci, V., Porfido, S., Cardinali, M., Violante, C., … Rossi, M. (2009). Central Italy seismic sequences- induced landsliding: 1997–1998 Umbria-Marche and 2008-2009 L'Aquila cases. In C.-Tyi Lee (Ed.), *The next generation of research on earthquake-induced landslides: An international conference in commemoration of 10th anniversary of the Chi-Chi earthquake, 2009*. Taoyuan County, Taiwan, National Central University.

Hancox, G., Perrin, N., & Dellow, G. (2002). Recent studies of historical earthquake-induced landsliding, ground damage, and MM intensity in New Zealand. *Bulletin of the New Zealand Society for Earthquake Engineering*, *35*(2), 59–95.

Hansen, A. (1984). Engineering geomorphology: The application of an evolutionary model of Hong Kong's terrain. *Zeitschrift fur Geomorphologie, N F Supplement band*, *51*, 39–50.

Harp, E. L., Hartzell, S. H., Jibson, R. W., Ramirez-Guzman, L., & Schmitt, R. G. (2014). Relation of landslides triggered by the Kiholo Bay earthquake to modeled ground motion. *Bulletin of the Seismological Society of America*, *104*(5), 2529–2540. https://doi.org/10.1785/0120140047

Harp, E. L., & Jibson, R. W. (1995). Inventory of landslides triggered by the 1994 Northridge, California earthquake (pp. 95–213). U.S. Geological Survey Open-File Report.

Harp, E. L., Jibson, R. W., & Schmitt, R. G. (2016). Map of landslides triggered by the January 12, 2010, Haiti earthquake, scientific investigations. (Map 3353, 15 p., 1 sheet, scale 1:150,000). Reston, VA: U.S. Geological Survey https://doi.org/10.3133/sim3353

Harp, E. L., & Keefer, D. K. (1990). Landslides triggered by the earthquake. In M. J. Rymer & W. L. Ellsworth (Eds.), *The Coalinga, California, earthquake of May 2, 1983* (pp. 335–347). U.S. Geological Survey Professional Paper.

Harp, E. L., Keefer, D. K., Sato, H. P., & Yagi, H. (2011). Landslide inventories: The essential part of seismic landslide hazard analyses. *Engineering Geology*, *122*(1–2), 9–21. https://doi.org/10.1016/j.enggeo.2010.06.013

Harp, E. L., Tanaka, K., Sarmiento, J., & Keefer, D. K. (1984). Landslides from the May 25–27, 1980, Mammoth Lakes, California, earthquake sequence (Map 1612, scale 1:62 500). U.S. Geological Survey Miscellaneous Investigations.

Harp, E. L., Wilson, R. C., & Wieczorek, G. F. (1981). *Landslides from the February 4, 1976, Guatemala earthquake*. Washington, DC: U.S. Government Printing Office.

Huang, R., & Fan, X. (2013). The landslide story. *Nature Geoscience*, *6*(5), 325–326. https://doi.org/10.1038/ngeo1806

Huang, T. F., & Lee, C. T. (1999). Landslides triggered by the Jueili earthquake. In *Proceedings of the 1999 Annual Meeting of the Geological Society of China*. Taipei.

Huang, R., & Li, W. (2009). Analysis of the geo-hazards triggered by the 12 May 2008 Wenchuan earthquake, China. *Bulletin of Engineering Geology and the Environment*, *68*(3), 363–371. https://doi.org/10.1007/s10064-009-0207-0

Jibson, R. W., & Harp, E. L. (2012). Extraordinary distance limits of landslides triggered by the 2011 mineral, Virginia, earthquake. *Bulletin of the Seismological Society of America*, *102*(6), 2368–2377. https://doi.org/10.1785/0120120055

Jibson, R. W., Harp, E. L., & Michael, J. A. (2000). A method for producing digital probabilistic seismic landslide hazard maps. *Engineering Geology*, *58*(3), 271–289. https://doi.org/10.1016/S0013-7952(00)00039-9

Jibson, R. W., Harp, E. L., Schulz, W., & Keefer, D. K. (2004). Landslides triggered by the 2002 Denali Fault, Alaska, earthquake and the inferred nature of the strong shaking. *Earthquake Spectra*, *20*(3), 669–691. https://doi.org/10.1193/1.1778173

Kargel, J. S., Leonard, G. J., Shugar, D. H., Haritashya, U. K., Bevington, A., Fielding, E. J., … Young, N. (2016). Geomorphic and geologic controls of geohazards induced by Nepal's 2015 Gorkha earthquake. *Science*, *351*(6269). https://doi.org/10.1126/science.aac8353

Keefer, D. K. (1984). Landslides caused by earthquakes. *Geological Society of America Bulletin*, *95*(4), 406–421. https://doi.org/10.1130/0016-7606(1984)95%3C406:LCBE%3E2.0.CO;2

Keefer, D. K. (2002). Investigating landslides caused by earthquakes—A historical review. *Surveys in Geophysics*, *23*(6), 473–510. https://doi.org/10.1023/A:1021274710840

Keefer, D. K., & Manson, M. W. (1998). Regional distribution and characteristics of landslides generated by the earthquake, In D. K. Keefer (Ed.), *The Loma Prieta, California, earthquakes of October 17, 1989-Landslides* (pp. 7–32). U.S. Geological Survey Professional Paper(1551-C).

Keefer, D. K., & Tannaci, N. E. (1981). Bibliography of landslides, soil liquefaction, and related ground failures in selected historic earthquakes (81–572). U.S. Geological Survey Open-File Report.

Kennedy, I. T., Petley, D. N., Williams, R., & Murray, V. (2015). A systematic review of the health impacts of mass earth movements (landslides). *PLOS Currents Disasters*, *7*. https://doi.org/10.1371/currents.dis.1d49e84c8bbe678b0e70cf7fc35d0b77

Klar, A., Aharonov, E., Kalderon-Asael, B., & Katz, O. (2011). Analytical and observational relations between landslide volume and surface area. *Journal of Geophysical Research*, *116*, F02001. https://doi.org/10.1029/2009JF001604

Kogyo, K. (2007). *Aerial photo interpretation of earthquake damage from the 2007 Niigata Chuetsu–oki earthquake*. Japan: Kokusai Kogyo Co., Ltd.

Korup, O. (2006). Effects of large deep-seated landslides on hillslope morphology, western Southern Alps, New Zealand. *Journal of Geophysical Research*, *111*, F01018. https://doi.org/10.1029/2004JF000242

Kritikos, T., Robinson, T. R., & Davies, T. R. (2015). Regional coseismic landslide hazard assessment without historical landslide inventories: A new approach. *Journal of Geophysical Research: Earth Surface*, *120*, 711–729. https://doi.org/10.1002/2014JF003224

Lacroix, P., Zavala, B., Berthier, E., & Audin, L. (2013). Supervised method of landslide inventory using panchromatic SPOT5 images and application to the earthquake-triggered landslides of Pisco (Peru, 2007, M_w8. 0). *Remote Sensing*, *5*(6), 2590–2616. https://doi.org/10.3390/rs5062590

Larsen, I. J., Montgomery, D. R., & Korup, O. (2010). Landslide erosion controlled by hillslope material. *Nature Geoscience*, *3*(4), 247–251. https://doi.org/10.1038/ngeo776

Lee, C.-T. (2014). Statistical seismic landslide hazard analysis: An example from Taiwan. *Engineering Geology*, *182*, 201–212. https://doi.org/10.1016/j.enggeo.2014.07.023

Li, W.-L., Huang, R.-Q., Xu, Q., & Tang, C. (2013). Rapid susceptibility mapping of co-seismic landslides triggered by the 2013 Lushan earthquake using the regression model developed for the 2008 Wenchuan earthquake. *Journal of Mountain Science*, *10*(5), 699–715. https://doi.org/10.1007/s11629-013-2786-2

Li, G., West, A. J., Densmore, A. L., Jin, Z., Parker, R. N., & Hilton, R. G. (2014). Seismic mountain building: Landslides associated with the 2008 Wenchuan earthquake in the context of a generalized model for earthquake volume balance. *Geochemistry, Geophysics, Geosystems*, *15*, 833–844. https://doi.org/10.1002/2013GC005067

Liao, H.-W., & Lee C.-T. (2000). Landslides triggered by the Chi-Chi earthquake. Paper presented at Proceedings of the 21st Asian conference on remote sensing.

Liu-Zeng, J., Wen, L., Oskin, M., & Zeng, L. (2011). Focused modern denudation of the Longmen Shan margin, eastern Tibetan Plateau. *Geochemistry, Geophysics, Geosystems*, *12*, Q11007. https://doi.org/10.1029/2011GC003652

Mahdavifar, M. R., Solaymani, S., & Jafari, M. K. (2006). Landslides triggered by the Avaj, Iran earthquake of June 22, 2002. *Engineering Geology*, *86*(2–3), 166–182. https://doi.org/10.1016/j.enggeo.2006.02.016

Malamud, B. D., Turcotte, D. L., Guzzetti, F., & Reichenbach, P. (2004a). Landslide inventories and their statistical properties. *Earth Surface Processes and Landforms*, *29*(6), 687–711. https://doi.org/10.1002/esp.1064

Malamud, B. D., Turcotte, D. L., Guzzetti, F., & Reichenbach, P. (2004b). Landslides, earthquakes, and erosion. *Earth and Planetary Science Letters*, *229*(1), 45–59. https://doi.org/10.1016/j.epsl.2004.10.018

Marano, K. D., Wald, D. J., & Allen, T. I. (2010). Global earthquake casualties due to secondary effects: A quantitative analysis for improving rapid loss analyses. *Natural Hazards*, *52*(2), 319–328. https://doi.org/10.1007/s11069-009-9372-5

Marc, O., & Hovius, N. (2015). Amalgamation in landslide maps: Effects and automatic detection. *Natural Hazards and Earth System Sciences*, *15*(4), 723–733. https://doi.org/10.5194/nhess-15-723-2015

Marc, O., Hovius, N., & Meunier, P. (2016). The mass balance of earthquakes and earthquake sequences. *Geophysical Research Letters*, *43*, 3708–3716. https://doi.org/10.1002/2016GL068333

Marc, O., Hovius, N., Meunier, P., Gorum, T., & Uchida, T. (2016). A seismologically consistent expression for the total area and volume of earthquake-triggered landsliding. *Journal of Geophysical Research: Earth Surface*, *121*, 640–663. https://doi.org/10.1002/2015JF00373

Martha, T. R., Kerle, N., Jetten, V., van Westen, C. J., & Kumar, K. V. (2010). Characterising spectral, spatial and morphometric properties of landslides for semi-automatic detection using object-oriented methods. *Geomorphology*, *116*(1–2), 24–36. https://doi.org/10.1016/j.geomorph.2009.10.004

Martino, S., Prestininzi, A., & Romeo, R. (2014). Earthquake-induced ground failures in Italy from a reviewed database. *Natural Hazards and Earth System Sciences*, *14*, 799–814. https://doi.org/10.5194/nhess-14-799-2014

Marui, H., & Nadim, F. (2009). Landslides and multi-hazards. In K. Sassa & P. Canuti (Eds.), *Landslides—Disaster risk reduction* (pp. 435–450). Berlin, Heidelberg: Springer Berlin Heidelberg. https://doi.org/10.1007/978-3-540-69970-5_23

Marzorati, S., Luzi, L., & De Amicis, M. (2002). Rock falls induced by earthquakes: A statistical approach. *Soil Dynamics and Earthquake Engineering*, *22*(7), 565–577. https://doi.org/10.1016/S0267-7261(02)00036-2

McCalpin, J. (1984). Preliminary age classification of landslides for inventory mapping. Paper presented at Proceedings 21st Engineering Geology and Soil Engineering Symposium, April.

McCrink, P. T. (2001). Regional earthquake-induced landslide mapping using Newmark displacement criteria. In H. Ferriz, & Anderson (Eds.), *Engineering Geology Practice in Northern California*, *Association of Engineering Geologists Special Publication 12* (Vol. 210, pp. 77–93). Santa Cruz County, CA: California Geological Survey Bulletin.

Meunier, P., Hovius, N., & Haines, J. A. (2008). Topographic site effects and the location of earthquake induced landslides. *Earth and Planetary Science Letters*, *275*(3–4), 221–232. https://doi.org/10.1016/j.epsl.2008.07.020

Ministerio de Medio Ambiente y Recursos Naturales (2001). Landslide inventory for the 2001 January 13 earthquake.

Morton, D. M. (1971). Seismically triggered landslides in the area above the San Fernando Valley, in the San Fernando, California, earthquake of February 9, 1971 (pp. 99–104). U.S. Geological Survey Professional Paper 733.

NASA Jet Propulsion Laboratory (JPL) (2013). NASA Shuttle Radar Topography Mission United States 1 arc second. NASA EOSDIS Land Processes DAAC, USGS Earth Resources Observation and Science (EROS) Center, Sioux Falls, South Dakota (https://lpdaac.usgs.gov), accessed January 1, 2015. https://doi.org/10.5067/MEaSUREs/SRTM/SRTMUS1.003

NIED (2016). Distribution map of mass movement by the 2016 Kumamoto earthquake, edited by National Research Institute for Earth Science and Disaster of Japan (in Japanese). Retrieved from http://www.bosai.go.jp/mizu/dosha.html

Nishida, K., Kobashi, S., & Mizuyama, T. (1996). Analysis of distribution of landslides caused by 1995 Hyogoken Nanbu earthquake referring to a database specialized for sediment related disasters (in Japanese with English abstract). *Journal of Japan Society of Erosion Control Engineering*, *49*(1), 19–24. https://doi.org/10.11475/sabo1973.49.19

Nowicki, M. A., Wald, D. J., Hamburger, M. W., Hearne, M., & Thompson, E. M. (2014). Development of a globally applicable model for near real-time prediction of seismically induced landslides. *Engineering Geology*, *173*, 54–65. https://doi.org/10.1016/j.enggeo.2014.02.002

Papadopoulos, G. A., & Plessa, A. (2000). Magnitude–distance relations for earthquake-induced landslides in Greece. *Engineering Geology*, *58*(3-4), 377–386. https://doi.org/10.1016/S0013-7952(00)00043-0

Papathanassiou, G., Valkaniotis, S., Ganas, A., & Pavlides, S. (2013). GIS-based statistical analysis of the spatial distribution of earthquake-induced landslides in the island of Lefkada, Ionian Islands, Greece. *Landslides*, *10*(6), 771–783. https://doi.org/10.1007/s10346-012-0357-1

Parker, R. N., Densmore, A. L., Rosser, N. J., de Michele, M., Li, Y., Huang, R., … Petley, D. N. (2011). Mass wasting triggered by the 2008 Wenchuan earthquake is greater than orogenic growth. *Nature Geoscience*, *4*(7), 449–452. https://doi.org/10.1038/ngeo1154

Parker, R., Hancox, G., Petley, D., Massey, C., Densmore, A., & Rosser, N. (2015). Spatial distributions of earthquake-induced landslides and hillslope preconditioning in the northwest South Island, New Zealand. *Earth Surface Dynamics*, *3*(4), 501–525. https://doi.org/10.5194/esurf-3-501-2015

Pašek, J. (1975). Landslides inventory. *Bulletin of the International Association of Engineering Geology - Bulletin de l'Association Internationale de Géologie de l'Ingénieur*, *12*(1), 73–74. https://doi.org/10.1007/bf02635432

Petley, D. (2012). Global patterns of loss of life from landslides. *Geology*, *40*(10), 927–930. https://doi.org/10.1130/G33217.1

Piacentini, T., Miccadei, E., Di Michele, R., Sciarra, N., & Mataloni, G. (2013). Geomorphological analysis applied to rock falls in Italy: The case of the San Venanzio gorges (Aterno River, Abruzzo, Italy). *Italian Journal of Engineering Geology and Environment*, *6*, 467–479. https://doi.org/10.4408/IJEGE.2013-06.B-45

Prestininzi, A., & Romeo, R. (2000). Earthquake-induced ground failures in Italy. *Engineering Geology*, *58*(3-4), 387–397. https://doi.org/10.1016/S0013-7952(00)00044-2

Qi, S., Xu, Q., Lan, H., Zhang, B., & Liu, J. (2010). Spatial distribution analysis of landslides triggered by 2008.5. 12 Wenchuan earthquake, China. *Engineering Geology*, *116*(1-2), 95–108. https://doi.org/10.1016/j.enggeo.2010.07.011

Roback, K., Clark, M. K., West, A. J., Zekkos, D., Li, G., Gallen, S. F., … Godt, J. W. (2017). Map data of landslides triggered by the 25 April 2015 M_w 7.8 Gorkha, Nepal earthquake. U.S. Geological Survey data release. https://doi.org/10.5066/F7DZ06F9

Robinson, T. R., Rosser, N. J., Densmore, A. L., Williams, J. G., Kincey, M. E., Benjamin, J., & Bell, H. J. A. (2017). Rapid post-earthquake modelling of coseismic landslide magnitude and distribution for emergency response decision support. *Natural hazards and earth system sciences discussions*, *2017*, 1–29. https://doi.org/10.5194/nhess-2017-83

Rodriguez, C., Bommer, J., & Chandler, R. (1999). Earthquake-induced landslides: 1980–1997. *Soil Dynamics and Earthquake Engineering*, *18*(5), 325–346. https://doi.org/10.1016/S0267-7261(99)00012-3

Rosser, B., Dellow, S., Haubrock, S., & Glassey, P. (2017). New Zealand's national landslide database. *Landslides*. https://doi.org/10.1007/s10346-017-0843-6

Rosser, B. J., Townsend, D., Mc Saveney, M., & Ries, W. (2014). Landslides and ground damage associated with the *M*6.2 Eketahuna earthquake, 20 January 2014, GNS Science Report.

Rymer, M. J. (1987). The San Salvador earthquake of October 10, 1986-geologic aspects. *Earthquake Spectra*, *3*(3), 435–463. https://doi.org/10.1193/1.1585440

Sappington, J., Longshore, K. M., & Thompson, D. B. (2007). Quantifying landscape ruggedness for animal habitat analysis: A case study using bighorn sheep in the Mojave desert. *The Journal of Wildlife Management*, *71*(5), 1419–1426. https://doi.org/10.2193/2005-723

Sato, H. P., Hasegawa, H., Fujiwara, S., Tobita, M., Koarai, M., Une, H., & Iwahashi, J. (2007). Interpretation of landslide distribution triggered by the 2005 northern Pakistan earthquake using SPOT 5 imagery. *Landslides*, *4*(2), 113–122. https://doi.org/10.1007/s10346-006-0069-5

Sato, H. P., Koarai, M., Une, H., Iwahashi, J., Miyahara, B., & Yamagishi, H. (2008). GIS analysis on geomorphological features of slope failures triggered by the Niigataken Chuetsu-oki earthquake in 2007 (in Japanese). *Journal of the Geographical Survey Institute of Japan*, *114*, 91–102. http://www.gsi.go.jp/common/000048571.pdf

Schlögel, R., Torgoev, I., De Marneffe, C., & Havenith, H. B. (2011). Evidence of a changing size–frequency distribution of landslides in the Kyrgyz Tien Shan, Central Asia. *Earth Surface Processes and Landforms*, *36*(12), 1658–1669. https://doi.org/10.1002/esp.2184

Schmitt, R. G., Tanyas, H., Nowicki Jessee, M. A., Zhu, J., Biegel, K. M., Allstadt, K. E., … Knudsen, K. L. (2017). An open repository of earthquake-triggered ground-failure inventories: U.S. Geological Survey data release collection. https://doi.org/10.5066/F7H70DB4

Sekiguchi, T., & Sato, H. P. (2006). Feature and distribution of landslides induced by the Mid Niigata prefecture earthquake in 2004, Japan. *Journal of the Japan Landslide Society*, *43*(3), 142–154. https://doi.org/10.3313/jls.43.142

Sepúlveda, S., Serey, A., Lara, M., Pavez, A., & Rebolledo, S. (2010). Landslides induced by the April 2007 Aysén Fjord earthquake, Chilean Patagonia. *Landslides*, *7*(4), 483–492. https://doi.org/10.1007/s10346-010-0203-2

Shafique, M., van der Meijde, M., & Khan, M. A. (2016). A review of the 2005 Kashmir earthquake-induced landslides; from a remote sensing prospective. *Journal of Asian Earth Sciences*, *118*, 68–80. https://doi.org/10.1016/j.jseaes.2016.01.002

Shieh, C. L., Chen, Y. S., Tsai, Y. J., & Wu, J. H. (2009). Variability in rainfall threshold for debris flow after the Chi-Chi earthquake in central Taiwan, China. *International Journal of Sediment Research*, *24*(2), 177–188. https://doi.org/10.1016/S1001-6279(09)60025-1

Stark, C. P., & Guzzetti, F. (2009). Landslide rupture and the probability distribution of mobilized debris volumes. *Journal of Geophysical Research: Earth Surface*, *114*, F00A02. https://doi.org/10.1029/2008JF001008

Suziki, K. (1979). On the disaster situation/land condition map of the Izu-Oshima Kinkai earthquake, 1978. *Journal of the Japan Cartographers Association*, *17*(2), 16–22. https://doi.org/10.11212/jjca1963.17.2_16

Tanaka, K. (1994). Landslides triggered by the earthquake—Case study of Okushiri Island affected by the Hokkaido Nansei Oki earthquake. In The Japan Landslide Society Branch (Ed.), *Landslides Triggered by the Earthquake*. Tokyo.

Tang, C., Westen, C. J. V., Tanyaş, H., & Jetten, V. G. (2016). Analyzing post-earthquake landslide activity using multi-temporal landslide inventories near the epicentral area of the 2008 Wenchuan earthquake. *Natural Hazards and Earth System Sciences*, *16*(12), 2641–2655. https://doi.org/10.5194/nhess-16-2641-2016

Uchida, T., Kataoka, S., Iwao, T., Matsuo, O., Terada, H., Nakano, Y., … Osanai, N. (2004). A study on methodology for assessing the potential of slope failures during earthquakes (in Japanese with English abstract). *Technical Note of National Institute for Land and Infrastructure Management, No.204,* (pp. 91). http://www.nilim.go.jp/lab/bcg/siryou/tnn/tnn0204.htm

Umar, Z., Pradhan, B., Ahmad, A., Jebur, M. N., & Tehrany, M. S. (2014). Earthquake induced landslide susceptibility mapping using an integrated ensemble frequency ratio and logistic regression models in west Sumatera Province, Indonesia. *Catena*, *118*, 124–135. https://doi.org/10.1016/j.catena.2014.02.005

Van Den Eeckhaut, M., Poesen, J., Govers, G., Verstraeten, G., & Demoulin, A. (2007). Characteristics of the size distribution of recent and historical landslides in a populated hilly region. *Earth and Planetary Science Letters*, *256*(3-4), 588–603. https://doi.org/10.1016/j.epsl.2007.01.040

Van Dissen, R., McSaveney, M., Townsend, D., Hancox, G., Little, T., Ries, W., … Massey, C. (2013). Landslides and liquefaction generated by the Cook Strait and Lake Grassmere earthquakes: A reconnaissance report. *Bulletin of the New Zealand Society for Earthquake Engineering*, *46*(4), 196–200.

Wald, D. J., Lin, K.-W., & Quitoriano, V. (2008). Quantifying and qualifying USGS ShakeMap uncertainty (pp. 26) U.S. Geological Survey Open File Report 2008–1238.

Wartman, J., Dunham, L., Tiwari, B., & Pradel, D. (2013). Landslides in eastern Honshu induced by the 2011 Tohoku earthquake. *Bulletin of the Seismological Society of America*, *103*(2B), 1503–1521. https://doi.org/10.1785/0120120128

Wasowski, J., Keefer, D. K., & Lee, C.-T. (2011). Toward the next generation of research on earthquake-induced landslides: Current issues and future challenges. *Engineering Geology*, *122*(1-2), 1–8. https://doi.org/10.1016/j.enggeo.2011.06.001

Wieczorek, G. F. (1984). Preparing a detailed landslide-inventory map for hazard evaluation and reduction. *Bulletin of the Association of Engineering Geologists*, *21*(3), 337–342.

Wilson, R., Wieczorek, G., Keefer, D., Harp, E., & Tannaci, N. (1985). Map showing ground failures from the Greenville/Mount Diablo earthquake sequence of January 1980, Northern California. Reston, VA: U.S. Geological Survey, Miscellaneous Field Studies Map.

Xu, C. (2014). Preparation of earthquake-triggered landslide inventory maps using remote sensing and GIS technologies: Principles and case studies. *Geoscience Frontiers*, *6*(6), 825–836. https://doi.org/10.1016/j.gsf.2014.03.004

Xu, C., Xu, X., & Shyu, J. B. H. (2015). Database and spatial distribution of landslides triggered by the Lushan, China M_w 6.6 earthquake of 20 April 2013. *Geomorphology*, *248*, 77–92. https://doi.org/10.1016/j.geomorph.2015.07.002

Xu, C., Xu, X., Shyu, J. B. H., Zheng, W., & Min, W. (2014). Landslides triggered by the 22 July 2013 Minxian–Zhangxian, China, M_w 5.9 earthquake: Inventory compiling and spatial distribution analysis. *Journal of Asian Earth Sciences*, *92*, 125–142. https://doi.org/10.1016/j.jseaes.2014.06.014

Xu, C., Xu, X., Yao, X., & Dai, F. (2014). Three (nearly) complete inventories of landslides triggered by the May 12, 2008 Wenchuan M_w 7.9 earthquake of China and their spatial distribution statistical analysis. *Landslides*, *11*(3), 441–461. https://doi.org/10.1007/s10346-013-0404-6

Xu, C., Xu, X., & Yu, G. (2013). Landslides triggered by slipping-fault-generated earthquake on a plateau: An example of the 14 April 2010, M_s 7.1, Yushu, China earthquake. *Landslides*, *10*(4), 421–431. https://doi.org/10.1007/s10346-012-0340-x

Yagi, H., Sato, G., Higaki, D., Yamamoto, M., & Yamasaki, T. (2009). Distribution and characteristics of landslides induced by the Iwate–Miyagi Nairiku earthquake in 2008 in Tohoku District, Northeast Japan. *Landslides*, *6*(4), 335–344. https://doi.org/10.1007/s10346-009-0182-3

Yagi, H., Yamasaki, T., & Atsumi, M. (2007). GIS analysis on geomorphological features and soil mechanical implication of landslides caused by 2004 Niigata Chuetsu earthquake. *Journal of the Japan Landslide Society*, *43*(5), 294–306. https://doi.org/10.3313/jls.43.294

Ying-ying, T., Chong, X., Xi-wei, X., Sai-er, W., & Jian, C. (2015). Spatial distribution analysis of coseismic and pre-earthquake landslides triggered by the 2014 Ludian MS6.5 earthquake. *Seismology and Geology*, *37*(1), 291–306. https://doi.org/10.3969/j.issn.0253-4967.2015.01.023

Zhang, J., Liu, R., Deng, W., Khanal, N. R., Gurung, D. R., Murthy, M. S. R., & Wahid, S. (2016). Characteristics of landslide in Koshi River basin, central Himalaya. *Journal of Mountain Science*, *13*(10), 1711–1722. https://doi.org/10.1007/s11629-016-4017-0